Sensors and Materials, Vol. 35, No. 7 (2023) 2457–2482
MYU Tokyo

S & M 3335

Adaptive Tracking Control of Single Input Single Output Nonlinear System with Sectorial Dead Zone Using Interval Type-2 Neural Network Fuzzy Control

Ho Sheng Chen,[1] Wen-Shyong Yu,[2] and Tian-Syung Lan[3*]

[1]School of Materials Science and Engineering, Guangdong University of Petrochemical Technology, 139 Guandu Road, Maonan District, Maoming, Guangdong Province 525000 China
[2]Department of Electrical Engineering, Tatung University, No. 40, Sec. 3, Zhongshan N. Rd., Taipei City 104, Taiwan
[3]Department of Information Management, Yu Da University of Science and Technology, No. 168, Hsueh-fu Rd., Tanwen Village, Chaochiao Township, Miaoli County, 361 Taiwan

(Received April 15, 2023; accepted July 4, 2023)

Keywords: SISO nonlinear system, interval Type-2 neural network fuzzy (IT2-NNF), Lyapunov stability criterion, H∞ tracking performance, Riccati inequality, sectorial dead zone

Single-input, single-output (SISO) nonlinear systems have problems with sectorial dead zone nonlinearities, noise, uncertainties, approximation errors, and external disturbances. Therefore, we developed an interval Type-2 neural network fuzzy adaptive controller (IT2-NNFAC) for satisfactory H-infinity (H_∞) tracking performance to solve the problems of the SISO system. To adjust the parameters of the proposed IT2-NNFAC, a structure of the fuzzy logic inference system and online adaptive laws are adopted, which are based on the Lyapunov stability criterion and Riccati inequality. All systems with the proposed IT2-NNFAC attenuate the effect of external disturbances on tracking errors at any specified level. In the proposed IT2-NNFAC, all the signals in the closed-loop system guarantee uniform and ultimate boundedness and satisfactory tracking performance with the proper Lyapunov stability criterion and Riccati inequality. H_∞ tracking responses and the resilience and efficacy of the proposed IT2-NNFAC were proved by testing a mass spring damper system with sectorial dead zone nonlinearities, uncertainties, and external disturbances.

1. Introduction

In machinery, the effect of dead zone nonlinearities needs to be estimated precisely as the nonlinearities cause instability in performance and reduce performance. Such nonlinearities are frequently encountered in valves and gears. Sensors are used to monitor acceleration and velocity and detect nonlinearities. To evaluate the effect of dead zone nonlinearities accurately, fuzzy control systems based on heuristic knowledge or linguistic information have been used for nonlinear systems since they do not require a precise mathematical model.(1) Adaptive fuzzy control based on the universal approximation theorem is used in nonlinear systems to acquire

*Corresponding author: e-mail: tslan888@yahoo.com.tw
https://doi.org/10.18494/SAM4454

ISSN 0914-4935
https://myukk.org/

data and modify the control parameters.[2,3] A robust compensator such as a sliding mode controller, a robust adaptive controller, or an H-infinity (H_∞) tracking controller is added to adaptive fuzzy controllers to mitigate external disturbances and fuzzy approximation errors.[4] However, dead zone nonlinearities occur often when using controllers in nonlinear systems, which reduce performance and cause instability.[5]

The dead zone nonlinearity is one of the serious nonsmooth nonlinearities in industrial processes. Thus, various adaptive control approaches have been proposed to solve the problems related to dead zone nonlinearities. For example, an adaptive neural technique was employed for unknown non-affine nonlinear systems with input dead zones and external unknown disturbances,[6] while dead zone inverses were presented for both linear and nonlinear systems with such problems to measure dead zone outputs.[7,8] An adaptive neural network (ANN) was used to control a quadruped robot with an unknown input dead zone.[9,10] For nonlinear systems with dead-zone input and output restrictions, unknown nonlinear canonical forms, and known maximum and minimum values, ANN tracking control was also applied using the backstepping technique and the identical slopes of the dead zone.[11–13] To solve nonlinearities and dead zone issues, fuzzy systems were also used. By focusing on the tracking issue, a nonlinear system that was mismatched and lacked recognized features due to dead zone flaws was explored.[14] For interconnected multiple input multiple output (MIMO) non-affine nonlinear systems, a fuzzy system with an observer-based interval Type-2 hierarchical fuzzy neural controller (OBIT2HFNC) was developed.[15] For nonlinear systems with uncertainties, a Type-2 fuzzy-neural network (T2FNN) with Petri networks and a novel universal approximator was proposed, and an interval T2FNN (IT2FNN) with a new robust and adaptive control mechanism was constructed.[16,17] In uncertain nonlinear systems with sector dead zone nonlinearities, a sliding mode controller was presented to ensure the reaching condition.[18] However, there is a need to stabilize the nonlinear system with dead zone nonlinearities, particularly when high-precision movement is required. Fuzzy control using heuristic knowledge or linguistic information has been adopted as an efficient method for controlling system parameters and minimizing the impact of unknown nonlinearities in a complex nonlinear system.[19–21] An adaptive fuzzy control for the uncertain MIMO system with dead zone and time-varying external disturbance was developed using the membership functions for the Type-1 fuzzy logic system (T1FLS) and ensuring stability.[22–24]

The nonlinear system contains parameter uncertainties as the membership functions in T1FLS are unknown. Owing to this problem, Lyapunov stability analyses are conservatively used but cause unstable situations with uncertainties. Therefore, Type-2 FLS (T2FLS) was developed to cope with membership grades that are unexpected in nonlinear dynamic systems. T2FLS is based on the extended idea of Type-1 FLS with the principal members of any subset in [0,1] and fuzzy membership functions.[25,26] The output processor, inference engine, rule base, and fuzzifier of T2FLS are identical to those in T1FLS. Additionally, by using a crisp set or a type reducer and defuzzifier, the output processor of T2FLS creates a Type-1 fuzzy set.[27] The crisp set has elements of binary values. Fuzzy neural networks (FNNs) are a combination of artificial neural networks and fuzzy reasoning and are used to manage uncertain input and learn from processes and mimic uncertain nonlinear systems. Because of this, much research has been

conducted on sophisticated controllers and complicated plant systems employing FNNs.[28–30] The T2FNN contains a linguistic process of T2FLS as the antecedent component and an interval neural network as the consequence part and exhibits better performance than the Type-1 FNN (T1FNN). It accelerates the computation of T1FNN and allows the employment of an interval Type-2 fuzzy linguistic process in the previous step. A three-layer interval in the follow-up step is used as a generic T2FNN due to its complexity which requires many computations. The advantage of T2FNN over T1FNN includes handling ambiguous membership function grades in a variety of applications such as adaptive filtering[31] and wheeled mobile robots.[32]

In this study, we propose a single input single output (SISO) nonlinear system with a newly developed interval Type-2 neural network fuzzy adaptive controller (IT2NNFAC). With the proposed system, H_∞ tracking performance is improved, and reduced the effects of sectorial dead zone nonlinearities in the control input and external disturbances. As a result, the tracking error caused by fuzzy approximation errors is reduced, which has not been successful with existing fuzzy adaptive controllers. By using the proper Lyapunov criterion and Riccati inequality, the SISO nonlinear system also reduces sectorial dead zone nonlinearities, uncertainties, and external disturbances and shows swift H_∞ tracking responses, resilience, and efficacy.[11,12,14,17,18,20,27]

2. Materials and Methods

IT2NNFAC with adaption capabilities is used in the uncertain SISO nonlinear system with sectorial dead zone input. IT2NNFAC is generated using the linear matrix inequality (LMI) toolbox of Matlab to ensure that all system states are constrained and to reduce the impact of external disturbances on the tracking error at any level.

2.1 Problem definition of SISO system

In considering a class of SISO uncertain nonlinear systems with sectorial dead zone input, the following expression for the systems is defined.

$$\begin{cases} \dot{x}_1 &= x_2 \\ \dot{x}_2 &= x_3 \\ &\vdots \\ \dot{x}_{n-1} &= x_n \\ \dot{x}_n &= F_\alpha(x) + F_\beta(x) + G\Phi(u) + d \\ y &= x_1 \end{cases} \tag{1}$$

Here, $\boldsymbol{x} = \left[x_1\ x_2\ \ldots\ x_n\right]^T \in \mathbb{R}^n$ is the system state vector, which is assumed to be available for measurement, $u \in \mathbb{R}$ and $\Phi(u) \in \mathbb{R}$ are the control input and output of the sectorial dead zone model, respectively, $y \in \mathbb{R}$ is the system output, $F_\alpha(x)$, $F_\beta(x)$ are unknown continuous nonlinear system functions, G is a constant, and d is the restricted external disturbance. Then, Eq. (1) is rewritten as

$$\dot{x} = \mathbf{A}x + \mathbf{B}\left(F_\alpha\left(x\right) + F_\beta\left(x\right) + G\Phi\left(u\right) + d\right), \tag{2}$$

where $\mathbf{A}=\begin{bmatrix} 0 & 1 & 0 & \cdots & 0 \\ 0 & 0 & 1 & \cdots & 0 \\ \vdots & \vdots & \vdots & \ddots & \vdots \\ 0 & 0 & 0 & \cdots & 1 \\ 0 & 0 & 0 & \cdots & 0 \end{bmatrix} \in \mathbb{R}^{n\times n}, \mathbf{B} = \begin{bmatrix} 0 & 0 & 0 \cdots & 1 \end{bmatrix}^T \in \mathbb{R}^{n\times 1}$.

2.2 Sectorial dead zone nonlinearity

Dead zone and interval dead zone are two types of input nonsmooth nonlinearities that may have an impact on the operation of mechanical systems. Since many physical systems have such nonlinearities, a sectorial dead zone is created to symbolize the combined dead zone and interval dead zone as illustrated in Fig. 1.

According to Fig. 2, the median, lower, and upper bounds of the immeasurable nonlinear continuous functions $\Phi\left(u\right)=\left[\underline{\Phi}\left(u\right)\ \ \overline{\Phi}\left(u\right)\right]$ with input u for $\Phi'\left(u\right)$, $\underline{\Phi}\left(u\right)$, and $\overline{\Phi}\left(u\right)$, have the following intervals.

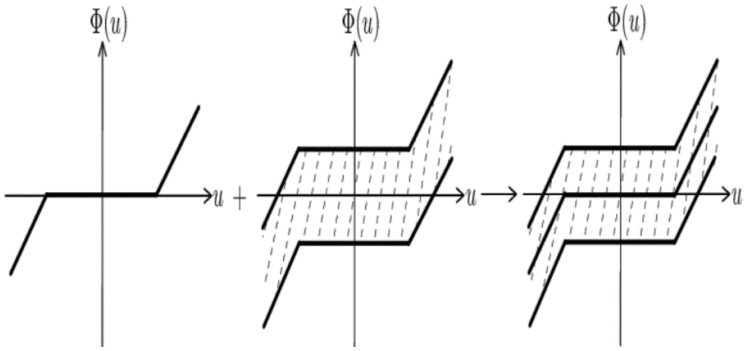

Fig. 1. Combination of dead zone and interval dead zone.

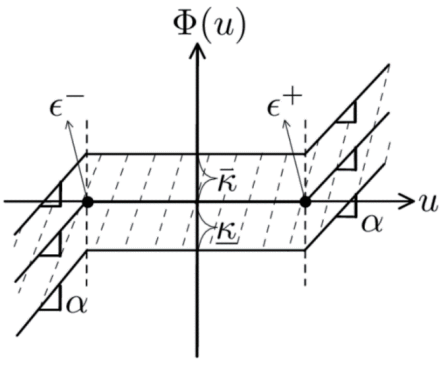

Fig. 2. Sectorial dead zone.

$$\Phi(u)=\begin{cases}\overline{\Phi}(u)=\begin{cases}\overline{\alpha}\left(u-\varepsilon^{+}\right)+\overline{\kappa}, & u\geq\varepsilon^{+} \text{ and } \overline{\Phi}(u)\geq\overline{\kappa}\\ \overline{\kappa}, & \varepsilon^{-}<u<\varepsilon^{+} \text{ and } 0<\overline{\Phi}(u)<\overline{\kappa}\\ \overline{\alpha}\left(u-\varepsilon^{-}\right)+\overline{\kappa}, & u\leq\varepsilon^{-} \text{ and } \overline{\Phi}(u)\leq\overline{\kappa}\end{cases}\\ \Phi'(u)=\begin{cases}\alpha'\left(u-\varepsilon^{+}\right), & u\geq\varepsilon^{+}\\ 0, & \varepsilon^{-}<u<\varepsilon^{+}\\ \alpha'\left(u-\varepsilon^{-}\right), & u\leq\varepsilon^{-}\end{cases}\\ \underline{\Phi}(u)=\begin{cases}\underline{\alpha}\left(u-\varepsilon^{+}\right)+\underline{\kappa}, & u\geq\varepsilon^{+} \text{ and } \underline{\Phi}(u)\geq\underline{\kappa}\\ \underline{\kappa}, & \varepsilon^{-}<u<\varepsilon^{+} \text{ and } \underline{\kappa}<\underline{\Phi}(u)<0\\ \underline{\alpha}\left(u-\varepsilon^{-}\right)+\underline{\kappa}. & u\leq\varepsilon^{-} \text{ and } \underline{\Phi}(u)\leq\underline{\kappa}\end{cases}\end{cases} \tag{3}$$

Here, α', $\underline{\alpha}$, and $\overline{\alpha}$ are the slopes of the sectorial dead zones $\Phi'(u)$, $\underline{\Phi}(u)$, and $\overline{\Phi}(u)$, respectively, and it is presumed that both positive and negative regions have the same value, i.e., $\alpha=\alpha'=\underline{\alpha}=\overline{\alpha}$, and ε^{-}, ε^{+}, $\underline{\kappa}$, and $\overline{\kappa}$ are sectorial dead zone envelopes that are constants. The following assumptions are suggested to acquire the essential characteristics of sectorial dead zone nonlinearities in the control issues.

2.2.1 Assumption 1

When $\varepsilon^{-}_{\max}$, $\varepsilon^{-}_{\min}$, $\varepsilon^{+}_{\max}$, $\varepsilon^{+}_{\min}$, $\underline{\kappa}_{\max}$, $\underline{\kappa}_{\min}$, $\overline{\kappa}_{\max}$, $\overline{\kappa}_{\min}$, $\alpha'_{\max}$, $\alpha'_{\min}$, $\underline{\alpha}_{\max}$, $\underline{\alpha}_{\min}$, $\overline{\alpha}_{\max}$, and $\overline{\alpha}_{\min}$ are constants, and ε^{-}, ε^{+}, $\underline{\kappa}$, $\overline{\kappa}$, α', $\underline{\alpha}$, and $\overline{\alpha}$ are unknown sectorial dead zone parameters, $\varepsilon^{-}\in\left\{\varepsilon^{-}_{\min},\varepsilon^{-}_{\max}\right\}$, $\varepsilon^{+}\in\left\{\varepsilon^{+}_{\min},\varepsilon^{+}_{\max}\right\}$, $\underline{\kappa}\in\left\{\underline{\kappa}_{\min},\underline{\kappa}_{\max}\right\}$, $\overline{\kappa}\in\left\{\overline{\kappa}_{\min},\overline{\kappa}_{\max}\right\}$, $\alpha'\in\left\{\alpha'_{\min},\alpha'_{\max}\right\}$, $\underline{\alpha}\in\left\{\underline{\alpha}_{min},\underline{\alpha}_{max}\right\}$, and $\overline{\alpha}\in\left\{\overline{\alpha}_{min},\overline{\alpha}_{max}\right\}$ are satisfied for which $\varepsilon^{+}_{\max}$, $\varepsilon^{-}_{\min}$, $\underline{\kappa}_{\max}$, and $\underline{\kappa}_{\min}$, are negative values and $\alpha'_{\min}$, $\underline{\alpha}_{\min}$, and $\overline{\alpha}_{\min}$ are nonzero.

In practice, on the basis of Assumption 1 and Eq. (3), it is possible to write the following equation.

$$\Phi(u)=\alpha u+\psi(u) \tag{4}$$

Here, $\psi(u)$ is determined using Eqs. (3) and (4) as follows.

$$\psi(u)=\begin{cases}-\alpha\varepsilon^{+}+\overline{\kappa}, & u\geq\varepsilon^{+}, \text{ and } \Phi(u)\geq\overline{\kappa}\\ -\alpha u+\kappa, & \varepsilon^{-}<u<\varepsilon^{+}, \text{ and } \underline{\kappa}<\Phi(u)<\overline{\kappa}\\ -\alpha\varepsilon^{-}+\underline{\kappa}, & u\leq\varepsilon^{-}. \text{ and } \Phi(u)\leq\underline{\kappa}\end{cases} \tag{5}$$

2.2.2 Assumption 2

According to the sectorial dead zone properties, $\psi(u)$ in Eq. (4) is bounded, which means that the positive constant is used as follows.

$$\rho = \max\left\{\left|\alpha_{\max}\varepsilon_{\max}^{+} + \overline{\kappa}_{\max}\right|, \left|\alpha_{\min}\varepsilon_{\min}^{-} + \underline{\kappa}_{\min}\right|\right\}$$

where $|\psi(u)| \leq \rho$.

Let $\boldsymbol{x}_m = \begin{bmatrix} x_{m_1} & x_{m_2} & \cdots & x_{m_n} \end{bmatrix}^T \in \mathbb{R}^n$ be the specified tracking reference signal with $\boldsymbol{x}_m(t) \in U_r$ for all $t \geq 0$ and for the desired compact set U_r. Tracking error is defined as $e = \boldsymbol{x} - \boldsymbol{x}_m = \begin{bmatrix} x_1 - x_{m_1} & x_2 - x_{m_2} & \cdots & x_n - x_{m_n} \end{bmatrix}^T = \begin{bmatrix} e_1 & e_2 & \ldots & e_n \end{bmatrix}^T$. Then, from Eqs. (2) and (4), the error dynamic equation can be written as

$$\dot{\boldsymbol{e}} = \mathbf{A}\boldsymbol{e} + \boldsymbol{B}\left(F_\alpha(\boldsymbol{x}) + F_\beta(\boldsymbol{x}) + \alpha G u + G\psi(u) + d - \boldsymbol{x}_d\right), \tag{6}$$

where $\boldsymbol{x}_d = \boldsymbol{x}_{m_n}$.

2.3 Model description of interval Type-2 neural network fuzzy (IT2NNF)

A fuzzy logic system (FLS) with a learning algorithm consists of four key components: fuzzifer, fuzzy rule base, fuzzy inference engine, and defuzzifer. IT2NNF has been used to solve uncertainty problems. In this section, the design process of IT2NNF is introduced.

The IF-THEN rules for an IT2NNF are expressed as follows.

$R_{F_\alpha}^{\ell}$: IF x_1 is $F_{F_{\alpha 1}}^{\ell}$ and x_2 is $F_{F_{\alpha 2}}^{\ell}$ and … and x_n is $F_{F_{\alpha n}}^{\ell}$, then y_{F_α} is $C_{F_\alpha}^{\ell}$.

$R_{F_\beta}^{\ell}$: IF x_1 is $F_{F_{\beta 1}}^{\ell}$ and x_2 is $F_{F_{\beta 2}}^{\ell}$ and … and x_n is $F_{F_{\beta n}}^{\ell}$, then y_{F_β} is $C_{F_\beta}^{\ell}$.

For l = 1, 2,..., p, where $F_{F_{\alpha i}}^{\ell}$, $F_{F_{\beta i}}^{\ell}$ and $C_{F_\alpha}^{\ell}$, $C_{F_\beta}^{\ell}$, $i = 1, 2, \ldots, n$, are inputs and outputs of T2FLS, respectively, $\mu_{F_{F_{\alpha i}}^{\ell}}(x_i)$, $\mu_{F_{F_{\beta i}}^{\ell}}(x_i)$, and $\mu_{C_{F_\alpha}^{\ell}}(\hat{y}_{F_\alpha})$, $\mu_{C_{F_\beta}^{\ell}}(\hat{y}_{F_\beta})$ are the functions of their corresponding memberships, and P is the total number of the Type-2 fuzzy rule. Figures 3 and 4 show the structure and detailed configuration of the proposed IT2NNF with the superscript indicating the layer number. IT2NNF is introduced layer by layer as follows.

2.3.1 Layer 1 (Input Layer)

This layer holds the inputs x_i, i = 1, 2,..., n of IT2NNF, which are designated as the state variables of Eq. (2).

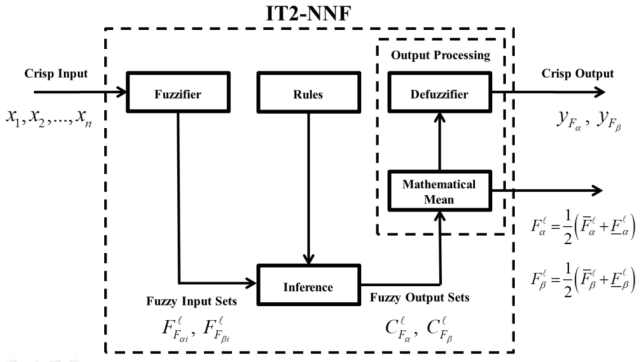

Fig. 3. Structure of proposed IT2NNF in this study.

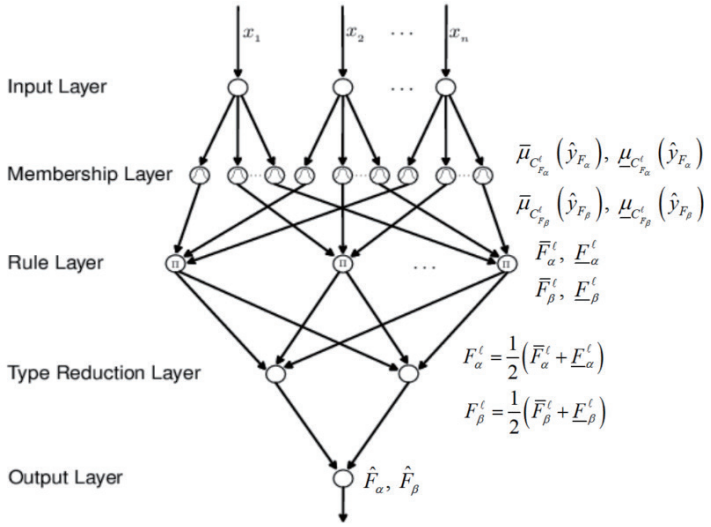

Fig. 4. Detailed configuration of proposed IT2NNF in this study.

2.3.2 Layer 2 (Membership Layer)

Each node in this layer works within the footprint of uncertainty (FOU), which is separated into upper and lower T1 membership functions, $\overline{\mu}_{C_{F_\alpha}^\ell}\left(\hat{y}_{F_\alpha}\right)$, $\overline{\mu}_{C_{F_\beta}^\ell}\left(\hat{y}_{F_\beta}\right)$, and $\underline{\mu}_{C_{F_\alpha}^\ell}\left(\hat{y}_{F_\alpha}\right)$, $\underline{\mu}_{C_{F_\beta}^\ell}\left(\hat{y}_{F_\beta}\right)$, respectively.

2.3.3 Layer 3 (Rule Layer)

The decision-making mechanism is the fuzzy inference engine. It employs fuzzy rules to compute the mapping of Type-2 fuzzy sets from input to output. The $F_\alpha^\ell \in C_{F_\alpha}^\ell$ and $F_\beta^\ell \in C_{F_\beta}^\ell$ firing intervals in Eqs. (13) and (14) are interval Type-2 fuzzy sets, values that are not crisp, and the intervals between $F_\alpha^\ell = \left[\underline{F}_\alpha^\ell \;\; \overline{F}_\alpha^\ell\right]$ and $F_\beta^\ell = \left[\underline{F}_\beta^\ell \;\; \overline{F}_\beta^\ell\right]$ are defined by the leftmost $\underline{F}_\alpha^\ell$, $\underline{F}_\beta^\ell$ and rightmost $\overline{F}_\alpha^\ell$, $\overline{F}_\beta^\ell$ points, respectively. The singleton fuzzifier and product inference are used to create the following equations.

$$\overline{F}_{\alpha}^{\ell} = \overline{\mu}_{C_{F_\alpha}^{\ell}}\left(\hat{y}_{F_\alpha}\right) \times \Pi_{i=1}^{n} \overline{\mu}_{F_{F_{\alpha i}}^{\ell}}\left(x_i\right), \ \underline{F}_{\alpha}^{\ell} = \underline{\mu}_{C_{F_\alpha}^{\ell}}\left(y_{F_\alpha}\right) \times \Pi_{i=1}^{n} \underline{\mu}_{F_{F_{\alpha i}}^{\ell}}\left(x_i\right) \tag{7}$$

$$\overline{F}_{\beta}^{\ell} = \overline{\mu}_{C_{F_\beta}^{\ell}}\left(\hat{y}_{F_\beta}\right) \times \Pi_{i=1}^{n} \overline{\mu}_{F_{F_{\beta i}}^{\ell}}\left(x_i\right), \ \underline{F}_{\beta}^{\ell} = \underline{\mu}_{C_{F_\beta}^{\ell}}\left(y_{F_\beta}\right) \times \Pi_{i=1}^{n} \underline{\mu}_{F_{F_{\beta i}}^{\ell}}\left(x_i\right) \tag{8}$$

As presented in Fig. 5, the Gaussian membership functions for x_n of the IT2-NNFAC are employed. The functions are as follows.

$$\overline{\mu}_{F_{F_{\alpha i}}^{\ell}}\left(x_i\right) = e^{-\left(\frac{x_i - m_{F_{\alpha i}}}{\overline{\sigma}_{F_{\alpha i}}}\right)^2}, \ \underline{\mu}_{F_{F_{\alpha i}}^{\ell}}\left(x_i\right) = a_{F_{\alpha i}} e^{-\left(\frac{x_i - m_{F_{\alpha i}}}{\underline{\sigma}_{F_{\alpha i}}}\right)^2} \tag{9}$$

$$\overline{\mu}_{F_{F_{\beta i}}^{\ell}}\left(x_i\right) = e^{-\left(\frac{x_i - m_{F_{\beta i}}}{\overline{\sigma}_{F_{\beta i}}}\right)^2}, \ \underline{\mu}_{F_{F_{\beta i}}^{\ell}}\left(x_i\right) = a_{F_{\beta i}} e^{-\left(\frac{x_i - m_{F_{\beta i}}}{\underline{\sigma}_{F_{\beta i}}}\right)^2} \tag{10}$$

where $\underline{\sigma}_{F_{\alpha i}}$, $\underline{\sigma}_{F_{\beta i}}$ in the lower limit and $\overline{\sigma}_{F_{\alpha i}}$, $\overline{\sigma}_{F_{\beta i}}$ in the upper limit are the fixed standard deviations of the membership functions in the form of $\mu_{F_{F_{\alpha i}}^{\ell}}\left(x_i\right)$, $\mu_{F_{F_{\beta i}}^{\ell}}\left(x_i\right)$, respectively. The FOU width coefficients between the membership functions are $a_{F_{\alpha i}}$ and $a_{F_{\beta i}}$, and the means of the T2FLS membership functions are $m_{F_{\alpha i}}$ and $m_{F_{\beta i}}$. These parameters are affected by $0 < a_{F_{\alpha i}} < 1$, $0 < a_{F_{\beta i}} < 1$, $\overline{\sigma}_{F_{\alpha i}} < \underline{\sigma}_{F_{\alpha i}}$, and $\overline{\sigma}_{F_{\beta i}} < \underline{\sigma}_{F_{\beta i}}$, $i = 1,2,\ldots,n$.

Owing to the output variables of the Type-2 fuzzy system, y_{F_α} and y_{F_β}, and their maximum values, $\mu_{C_{F_\alpha}^{\ell}}\left(y_{F_\alpha}\right)$ and $\mu_{C_{F_\beta}^{\ell}}\left(y_{F_\beta}\right)$, are both expressed in $\hat{y}_{F_\alpha}$ and $\hat{y}_{F_\beta}$, and the membership functions of the ensuing fuzzy set, $\mu_{C_{F_\alpha}^{\ell}}\left(\hat{y}_{F_\alpha}\right)$ and $\mu_{C_{F_\beta}^{\ell}}\left(\hat{y}_{F_\beta}\right)$. We reduce the complexity of the membership functions without sacrificing generality as $\overline{\mu}_{C_{F_\alpha}^{\ell}}\left(\hat{y}_{F_\alpha}\right) = 1$. $\underline{\mu}_{C_{F_\alpha}^{\ell}}\left(\hat{y}_{F_\alpha}\right) = b_{F_\alpha}$,

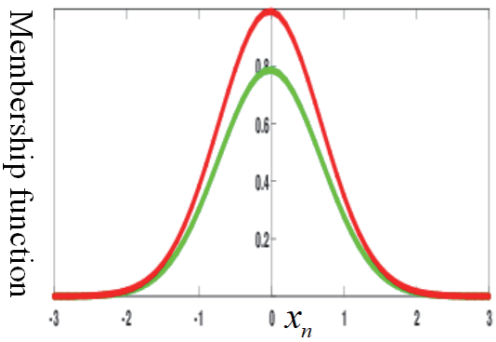

Fig. 5. (Color online) Membership function (x^i, $i = 1,2,\ldots,n$) of proposed IT2NNF.

$0 < b_{F_\alpha} < 1$ and $\overline{\mu}_{C^\ell_{F_\beta}}\left(\hat{y}_{F_\beta}\right) = 1$, $\underline{\mu}_{C^\ell_{F_\beta}}\left(\hat{y}_{F_\beta}\right) = b_{F_\beta}$, $0 < b_{F_\beta} < 1$ are the coefficients for the fuzzy set membership function's FOU width. With these, Eqs. (7) and (8) are revised to Eqs. (11) and (12).

$$\overline{F}^\ell_\alpha = 1 \times \Pi^n_{i=1} \overline{\mu}_{F^\ell_{F_{\alpha i}}}\left(x_i\right),\ \underline{F}^\ell_\alpha = b_{F_\alpha} \times \Pi^n_{i=1} \underline{\mu}_{F^\ell_{F_{\alpha i}}}\left(x_i\right) \tag{11}$$

$$\overline{F}^\ell_\beta = 1 \times \Pi^n_{i=1} \overline{\mu}_{F^\ell_{F_{\beta i}}}\left(x_i\right),\ \underline{F}^\ell_\beta = b_{F_\beta} \times \Pi^n_{i=1} \underline{\mu}_{F^\ell_{F_{\beta i}}}\left(x_i\right) \tag{12}$$

2.3.4 Layer 4 (Type Reduction Layer)

The type reduction is implemented using this layer. In contrast to T1FLS, T2FLS structure implementation is applied to the operations of fuzzification, inference, and output processing with type reduction and defuzzification.[33,34] The mathematical mean of the defuzzified outputs F^ℓ_α and F^ℓ is replaced with $F^\ell_\alpha = \frac{1}{2}\left(\overline{F}^\ell_\alpha + \underline{F}^\ell_\alpha\right)$ and $F^\ell_\beta = \frac{1}{2}\left(\overline{F}^\ell_\beta + \underline{F}^\ell_\beta\right)$ in T2FLS type reduction, which is an enhanced form of Type-1 defuzzification. The proposed IT2NNFAC becomes more computationally difficult as a result of the replacement, but it has the advantage of leveraging fuzzy set membership functions to address the inherent uncertainties in linguistic words.

2.3.5 Layer 5 (Output Layer)

The crisp outputs of T2FLS are used to approximate $F_\alpha(x)$ and $F_\beta(x)$ after the type-reduced sets have been defuzzified as follows.

$$\hat{F}_\alpha\left(x, \hat{\boldsymbol{\theta}}_{F_\alpha}\right) = \frac{\sum_{\ell=1}^{p} F^\ell_\alpha \hat{y}^\ell_\alpha}{\sum_{\ell=1}^{p} F^\ell_\alpha} = \xi^T_{F_\alpha}(x)\hat{\boldsymbol{\theta}}_{F_\alpha} \tag{13}$$

$$F_\beta\left(x, \boldsymbol{\theta}_{F_\beta}\right) = \frac{\sum_{\ell=1}^{p} F^\ell_\beta y^\ell_\beta}{\sum_{\ell=1}^{p} F^\ell_\beta} = \xi^T_{F_\beta}(x)\hat{\boldsymbol{\theta}}_{F_\beta} \tag{14}$$

Here, $\hat{\boldsymbol{\theta}}_{F_\alpha} = \left[\hat{\theta}^1_{F_\alpha}\ \hat{\theta}^2_{F_\alpha}\ \ldots\ \hat{\theta}^p_{F_\alpha}\right]^T$ and $\hat{\boldsymbol{\theta}}_{F_\beta} = \left[\hat{\theta}^1_{F_\beta}\ \hat{\theta}^2_{F_\beta}\ \ldots\ \hat{\theta}^p_{F_\beta}\right]^T$ are the adjustable parameter vectors, and $\boldsymbol{\xi}_{F_\alpha}(x) = \left[\xi^1_{F_\alpha}(x)\ \xi^2_{F_\alpha}(x)\ \cdots\ \xi^p_{F_\alpha}(x)\right]^T$ and $\boldsymbol{\xi}_{F_\beta}(x) = \left[\xi^1_{F_\beta}(x)\ \xi^2_{F_\beta}(x)\ \cdots\ \xi^p_{F_\beta}(x)\right]^T$ are the vectors of the fuzzy basis functions.

Additionally, the optimal approximation parameters $\boldsymbol{\theta}^*_{F_\alpha}$ and $\boldsymbol{\theta}^*_{F_\beta}$ are specified as follows by the universal approximation theorem.[35]

$$\boldsymbol{\theta}_{F_\alpha}^{*} = \arg\min_{\hat{\boldsymbol{\theta}}_{F_\alpha} \in \Omega_{F_\alpha}} \left\{ \sup_{x \in} \left\| \hat{F}_\alpha \left(x, \hat{\boldsymbol{\theta}}_{F_\alpha} \right) - F_\alpha(x) \right\| \right\} \tag{15}$$

$$\boldsymbol{\theta}_{F_\beta}^{*} = \arg\min_{\hat{\boldsymbol{\theta}}_{F_\beta} \in \Omega_{F_\beta}} \left\{ \sup_{x \in \mathbb{R}^n} \left\| \hat{F}_\beta \left(x, \hat{\boldsymbol{\theta}}_{F_\beta} \right) - F_\beta(x) \right\| \right\} \tag{16}$$

The minimum approximation errors for $F_\alpha(x)$ and $F_\beta(x)$ are defined as

$$\tilde{F}_\alpha = F_\alpha(x) - \hat{F}_\alpha \left(x, \boldsymbol{\theta}_{F_\alpha}^{*} \right), \tag{17}$$

$$\tilde{F}_\beta = F_\beta(x) - \hat{F}_\beta \left(x, \boldsymbol{\theta}_{F_\beta}^{*} \right), \tag{18}$$

where the minimum approximation errors are assumed to be constrained and are denoted by $\tilde{F}_\alpha$ and $\tilde{F}_\beta$. Accordingly, the estimated parameter errors are expressed as

$$\tilde{\boldsymbol{\theta}}_{F_\alpha} = \boldsymbol{\theta}_{F_\alpha}^{*} - \hat{\boldsymbol{\theta}}_{F_\alpha}, \tag{19}$$

$$\tilde{\boldsymbol{\theta}}_{F_\beta} = \boldsymbol{\theta}_{F_\beta}^{*} - \hat{\boldsymbol{\theta}}_{F_\beta}. \tag{20}$$

As a result, T2FLS is used to approximate the unknown functions F_α and F_β of the nonlinear controlled system in Eq. (2).

2.3.6 Assumption 3

When $\left| \left(\tilde{F}_\alpha + \tilde{F}_\beta \right)_i \right| \le M_e$, where $\left| (\cdot)_i \right|$ is the absolute value of the ith element of $\tilde{F}_\alpha + \tilde{F}_\beta$, $i = 1,2,...,n$, $M_e > 0$ with a positive constant.

3. Design of IT2NNFAC and Stability Analysis of SISO Nonlinear System

3.1 Design of IT2NNFAC

The unknown nonlinear functions $F_\alpha(x)$ and $F_\beta(x)$ are approximated by the Type-2 fuzzy universal approximators of $\hat{F}_\alpha \left(x, \hat{\boldsymbol{\theta}}_{F_\alpha} \right)$ and $\hat{F}_\beta \left(x, \hat{\boldsymbol{\theta}}_{F_\beta} \right)$, respectively, and IT2NNFAC is used to produce the output following a reference trajectory x_m. The proposed IT2NNFAC is given as follows from Assumptions 1 and 2 for sectorial dead zone nonlinearity.

$$u = (\alpha G)^{-1} \left(-\hat{F}_\alpha \left(x, \hat{\boldsymbol{\theta}}_{F_\alpha} \right) - \hat{F}_\beta \left(x, \hat{\boldsymbol{\theta}}_{F_\beta} \right) - G\rho + x_d - \mathbf{k}^T \mathbf{e} + u_h + u_\varepsilon \right) \tag{21}$$

Here, the characteristic polynomial of $\mathbf{A}_m = \mathbf{A} - \mathbf{B}\mathbf{k}^T$ is selected to be a Hurwitz matrix, $\boldsymbol{k}^T = \begin{bmatrix} k_1 & k_2 & \cdots & k_n \end{bmatrix}$ is the gain matrix, u_h and u_ε are used to compensate the approximation errors and the H_∞ robust control, and $\left|\psi(u)\right| \le \rho$ is described as Assumption 2.

Then, once $\mathbf{A}_\mathrm{m} = \begin{bmatrix} 0 & 1 & 0 & \cdots & 0 \\ 0 & 0 & 1 & \cdots & 0 \\ \vdots & \vdots & \vdots & \ddots & \vdots \\ 0 & 0 & 0 & \cdots & 1 \\ -k_1 & -k_2 & -k_3 & \cdots & -k_n \end{bmatrix}$ is defined, the error dynamics in Eq. (6) is transformed into

$$\dot{\mathbf{e}} = \mathbf{A}_\mathbf{m}\mathbf{e} + \mathbf{B}(F_\alpha(x) + F_\beta(x)) + \alpha G u + G\rho + d - x_d + \mathbf{k}^T\mathbf{e}). \tag{22}$$

Therefore, the error dynamics is obtained by substituting Eq. (21) into Eq. (22) as follows.

$$\begin{aligned} \dot{\mathbf{e}} &= \mathbf{A}_\mathbf{m}\mathbf{e} + \mathbf{B}\left(F_\alpha(x) - \hat{F}_\alpha\left(x, \hat{\boldsymbol{\theta}}_{F_\alpha}\right) + F_\beta(x) - F_\beta\left(x, \boldsymbol{\theta}_{F_\beta}\right) + d + u_h + u_\varepsilon \right) \\ &= \mathbf{A}_\mathbf{m}\mathbf{e} + \mathbf{B}\left(-\boldsymbol{\xi}_{F_\alpha}^T(\boldsymbol{x})\tilde{\boldsymbol{\theta}}_{F_\alpha} - \boldsymbol{\xi}_{F_\beta}^T(x)\tilde{\boldsymbol{\theta}}_{F_\beta} + \tilde{F}_\alpha + \tilde{F}_\beta + d + u_h + u_\varepsilon \right) \end{aligned} \tag{23}$$

3.1.1 Theorem 1

H_∞ performance is taken into account as follows.[36]

$$\int_0^{t_f} \mathbf{e}^\mathrm{T}\mathbf{Q}\mathbf{e}dt \le 2\mathbf{e}(0)^T\,\mathbf{P}\mathbf{e}(0) + \eta^2 \int_0^{t_f} \left(d^T d\right)dt \tag{24}$$

Here, the weighting matrix $\boldsymbol{Q} > 0$, $\boldsymbol{P} = \boldsymbol{P}^T > 0$, and η^2 denotes a prescribed attenuation level, which depicts the worst-case scenario of the tracking error e affected by the external disturbances d. No matter what d is, the effect on e must be reduced below a desired level η in terms of energy according to the physical definition of performance in Eq. (24). That is, a prescribed value η must be equal to or less than the L_2-gain from d to $\mathbf{e}$. For d, η is typically chosen as a positive small value less than one.

3.1.2 Theorem 2

The sectorial dead zone nonlinearities $\Phi(u)$ and uncertain nonlinear functions $F_\alpha(x)$ and $F_\beta(x)$ are taken into account for the controlled system [Eq. (2)]. The definition of IT2NNFAC with Eq. (21) is as follows.

$$u_h = -\frac{1}{\gamma}\boldsymbol{B}^T\boldsymbol{P}\boldsymbol{e} \tag{25}$$

$$u_{\varepsilon} = -M_e \operatorname{sgn}(\mathbf{B}^{\mathrm{T}}\mathbf{P}\mathbf{e}) \tag{26}$$

Here, the gain parameter $\operatorname{sgn}(\mathbf{B}^{\mathrm{T}}\mathbf{P}\mathbf{e}) = \begin{cases} 1, \text{ if } \mathbf{B}^{\mathrm{T}}\mathbf{P}\mathbf{e} \geq 0 \\ -1, \text{ if } \mathbf{B}^{\mathrm{T}}\mathbf{P}\mathbf{e} < 0 \end{cases}$, $\gamma > 0$. On the basis of Assumption 3, M_e is defined, and the symmetric positive definite matrix $\boldsymbol{P} = \boldsymbol{P}^{\mathrm{T}} > 0$ is obtained using the Matlab LMI toolbox according to the following Riccati-like equation.

$$\mathbf{A}_m^{\mathrm{T}}\mathbf{P} + \mathbf{P}\mathbf{A}_m + \mathbf{Q} + (-\frac{2}{\gamma} + \frac{1}{\eta^2})\mathbf{P}\mathbf{B}\mathbf{B}^{\mathrm{T}}\mathbf{P} \leq 0 \tag{27}$$

Here, a prescribed weighting matrix and a prescribed attenuation level are represented by $\boldsymbol{Q} = \boldsymbol{Q}^T \geq 0$ and $0 < \eta < 1$, respectively. The selected adaptive laws for adjusting the unknown SISO nonlinear system functions in IT2NNF are as follows.

$$\dot{\hat{\theta}}_{F_\alpha} = \gamma_{F_\alpha}\xi_{F_\alpha}(\boldsymbol{x})\boldsymbol{B}^{\mathrm{T}}\boldsymbol{P}\boldsymbol{e} \tag{28}$$

$$\dot{\hat{\theta}}_{F_\beta} = \gamma_{F_\beta}\xi_{F_\beta}(\boldsymbol{x})\boldsymbol{B}^{\mathrm{T}}\boldsymbol{P}\boldsymbol{e} \tag{29}$$

Here, the adaptation rates are $\gamma_{F_\alpha} > 0$ and $\gamma_{F_\beta} > 0$. The H_∞ tracking performance is then achieved within a specified value η^2 in the presence of external disturbances for any $t \geq 0$, $\boldsymbol{e}$, $\tilde{\theta}_{F_\alpha}$, and $\tilde{\theta}_{F_\beta}$ that are bounded.

3.2 Stability analysis of SISO nonlinear system

3.2.1 Proof 1

The candidate of the Lyapunov function is defined as

$$V = \frac{1}{2}\left(\mathbf{e}^{\mathrm{T}}\mathbf{P}\mathbf{e} + \frac{1}{\gamma_{F_\alpha}}\tilde{\theta}_{F_\alpha}^{\mathrm{T}}\tilde{\theta}_{F_\alpha} + \frac{1}{\gamma_{F_\beta}}\tilde{\theta}_{F_\beta}^{\mathrm{T}}\tilde{\theta}_{F_\beta}\right). \tag{30}$$

Taking a time derivative of Eq. (30),

$$\dot{V} = \frac{1}{2}\left(\dot{\mathbf{e}}^{\mathrm{T}}\mathbf{P}\mathbf{e} + \mathbf{e}^{\mathrm{T}}\mathbf{P}\dot{\mathbf{e}} + \frac{1}{\gamma_{F_\alpha}}\left(\dot{\tilde{\theta}}_{F_\alpha}^{\mathrm{T}}\tilde{\theta}_{F_\alpha} + \tilde{\theta}_{F_\alpha}^{\mathrm{T}}\dot{\tilde{\theta}}_{F_\alpha}\right) + \frac{1}{\gamma_{F_\beta}}\left(\dot{\tilde{\theta}}_{F_\beta}^{\mathrm{T}}\tilde{\theta}_{F_\beta} + \tilde{\theta}_{F_\beta}^{\mathrm{T}}\dot{\tilde{\theta}}_{F_\beta}\right)\right). \tag{31}$$

With $\dot{\tilde{\theta}}_{F_\alpha} = \dot{\hat{\theta}}_{F_\alpha}$, $\dot{\tilde{\theta}}_{F_\beta} = \dot{\hat{\theta}}_{F_\beta}$, substituting Eqs. (23) and (25) into Eq. (31) results in

$$\begin{aligned}\dot{V} = &\frac{1}{2}\left(\mathbf{A}_m\mathbf{e} + \mathbf{B}\left(-\boldsymbol{\xi}_{F_\alpha}^{\mathrm{T}}(\boldsymbol{x})\tilde{\boldsymbol{\theta}}_{F_\alpha} - \boldsymbol{\xi}_{F_\beta}^{\mathrm{T}}(\boldsymbol{x})\tilde{\boldsymbol{\theta}}_{F_\beta} + \tilde{F}_\alpha + \tilde{F}_\beta + d + u_h + u_\varepsilon\right)\right)^{\mathrm{T}}\mathbf{P}\mathbf{e} \\ &+ \frac{1}{2}\mathbf{e}^{\mathrm{T}}\mathbf{P}\left(\mathbf{A}_m\mathbf{e} + \mathbf{B}\left(-\boldsymbol{\xi}_{F_\alpha}^{\mathrm{T}}(\boldsymbol{x})\tilde{\boldsymbol{\theta}}_{F_\alpha} - \boldsymbol{\xi}_{F_\beta}^{\mathrm{T}}(\boldsymbol{x})\tilde{\boldsymbol{\theta}}_{F_\beta} + \tilde{F}_\alpha + \tilde{F}_\beta + d + u_h + u_\varepsilon\right)\right) \\ &+ \frac{1}{\gamma_{F_\alpha}}\tilde{\boldsymbol{\theta}}_{F_\alpha}^{\mathrm{T}}\dot{\tilde{\boldsymbol{\theta}}}_{F_\alpha} + \frac{1}{\gamma_{F_\beta}}\tilde{\boldsymbol{\theta}}_{F_\beta}^{\mathrm{T}}\dot{\tilde{\boldsymbol{\theta}}}_{F_\beta},\end{aligned} \tag{32}$$

$$\begin{aligned}= &\frac{1}{2}\mathbf{e}^{\mathrm{T}}\left(\mathbf{A}_{\mathrm{m}}^{\mathrm{T}}\mathbf{P} + \mathbf{P}\mathbf{A}_{\mathrm{m}} + \left(-\frac{2}{\gamma} + \frac{1}{\eta^2}\right)\mathbf{P}\mathbf{B}\mathbf{B}^{\mathrm{T}}\mathbf{P}\right)\mathbf{e} + \frac{1}{2}\eta^2 d^{\mathrm{T}}d \\ &- \frac{1}{2}\left(\frac{1}{\eta}\mathbf{B}^{\mathrm{T}}\mathbf{P}\mathbf{e} - \eta d\right)^{\mathrm{T}}\left(\frac{1}{\eta}\mathbf{B}^{\mathrm{T}}\mathbf{P}\mathbf{e} - \eta d\right) \\ &+ \mathbf{e}^{\mathrm{T}}\mathbf{P}\mathbf{B}\left(-\boldsymbol{\xi}_{F_\alpha}^{\mathrm{T}}(\boldsymbol{x})\tilde{\boldsymbol{\theta}}_{F_\alpha} - \boldsymbol{\xi}_{F_\beta}^{\mathrm{T}}(\boldsymbol{x})\tilde{\boldsymbol{\theta}}_{F_\beta} + \tilde{F}_\alpha + \tilde{F}_\beta + u_\varepsilon\right) \\ &+ \frac{1}{\gamma_{F_\alpha}}\tilde{\boldsymbol{\theta}}_{F_\alpha}^{\mathrm{T}}\dot{\tilde{\boldsymbol{\theta}}}_{F_\alpha} + \frac{1}{\gamma_{F_\beta}}\tilde{\boldsymbol{\theta}}_{F_\beta}^{\mathrm{T}}\dot{\tilde{\boldsymbol{\theta}}}_{F_\beta}.\end{aligned} \tag{33}$$

Applying the Riccati inequality [Eq. (27)] and the update laws and substituting Eqs. (28) and (29) into Eq. (33) result in

$$\begin{aligned}\dot{V} \le &-\frac{1}{2}\mathbf{e}^{\mathrm{T}}\mathbf{Q}\mathbf{e} + \frac{1}{2}\eta^2 d^{\mathrm{T}}d \\ &+ \frac{1}{\gamma_{F_\alpha}}\tilde{\boldsymbol{\theta}}_{F_\alpha}^{\mathrm{T}}\gamma_{F_\alpha}\boldsymbol{\xi}_{F_\alpha}(\boldsymbol{x})\mathbf{B}^{\mathrm{T}}\mathbf{P}\mathbf{e} + \frac{1}{\gamma_{F_\beta}}\tilde{\boldsymbol{\theta}}_{F_\beta}^{\mathrm{T}}\gamma_{F_\beta}\boldsymbol{\xi}_{F_\beta}(\boldsymbol{x})\mathbf{B}^{\mathrm{T}}\mathbf{P}\mathbf{e} \\ &- \tilde{\boldsymbol{\theta}}_{F_\alpha}^{\mathrm{T}}\boldsymbol{\xi}_{F_\alpha}(\boldsymbol{x})\mathbf{B}^{\mathrm{T}}\mathbf{P}\mathbf{e} - \tilde{\boldsymbol{\theta}}_{F_\beta}^{\mathrm{T}}\boldsymbol{\xi}_{F_\beta}(\boldsymbol{x})\mathbf{B}^{\mathrm{T}}\mathbf{P}\mathbf{e} + \mathbf{e}^{\mathrm{T}}\mathbf{P}\mathbf{B}\left(\tilde{F}_\alpha + \tilde{F}_\beta\right) + \mathbf{e}^{\mathrm{T}}\mathbf{P}\mathbf{B}u_\varepsilon.\end{aligned} \tag{34}$$

From Eq. (26), we have the following equation from Eq. (34).

$$\begin{aligned}\dot{V} &\le -\frac{1}{2}\mathbf{e}^{\mathrm{T}}\mathbf{Q}\mathbf{e} + \frac{1}{2}\eta^2 d^{\mathrm{T}}d + \mathbf{e}^{\mathrm{T}}\mathbf{P}\mathbf{B}\left(\tilde{F}_\alpha + \tilde{F}_\beta\right) - \mathbf{e}^{\mathrm{T}}\mathbf{P}\mathbf{B}M_e(x)\operatorname{sgn}\left(\mathbf{B}^{\mathrm{T}}\mathbf{P}\mathbf{e}\right) \\ &\le -\frac{1}{2}\mathbf{e}^{\mathrm{T}}\mathbf{Q}\mathbf{e} + \frac{1}{2}\eta^2 d^{\mathrm{T}}d + M_e(x)\left\|\mathbf{e}^{\mathrm{T}}\mathbf{P}\mathbf{B}\right\| - M_e(x)\left\|\mathbf{e}^{\mathrm{T}}\mathbf{P}\mathbf{B}\right\| \\ &\le -\frac{1}{2}\mathbf{e}^{\mathrm{T}}\mathbf{Q}\mathbf{e} + \frac{1}{2}\eta^2 d^{\mathrm{T}}d.\end{aligned} \tag{35}$$

Therefore,

$$\|\mathbf{e}\| \ge \frac{\eta\sqrt{d^{\mathrm{T}}d}}{\lambda_{min}(\mathbf{Q})}. \tag{36}$$

With respect to $\dot{V} \le 0$, $\lambda_{min}(\mathbf{Q})$ stands for the minimal eigenvalue of **Q**. The retarded functional differential equation is examined using the Lyapunov stability theory.[33,37] All realizations of uncertainties are guaranteed to be within the boundary of e and x_m, as well as the parameter estimation errors $\tilde{\boldsymbol{\theta}}_{F_\alpha}$ and $\tilde{\boldsymbol{\theta}}_{F_\beta}$, since η is the designed constant acting as an attenuation level.[34] Equations (35) and (36) at $t = 0$ to $t = t_f$ are integrated for $t \ge 0$. Then,

$$2V(t_f) - 2V(0) \le -\int_0^{t_f} \mathbf{e}^{\mathrm{T}}(t)\mathbf{Q}\mathbf{e}(t)dt + \eta^2 \int_0^{t_f} d^{\mathrm{T}}(t)d(t)dt \tag{37}$$

Since $V(t_f) \ge 0$, the inequality of Eq. (37) implies the following.

$$\begin{aligned}\int_0^{t_f} \mathbf{e}^{\mathrm{T}}(t)\mathbf{Q}\mathbf{e}(t)dt \le 2\mathbf{e}^{\mathrm{T}}(0)\mathbf{P}\mathbf{e}(0) &+ \frac{2}{\gamma_{F_\alpha}}\tilde{\boldsymbol{\theta}}_{F_\alpha}^{\mathrm{T}}(0)\tilde{\boldsymbol{\theta}}_{F_\alpha}(0) \\ &+ \frac{2}{\gamma_{F_\beta}}\tilde{\boldsymbol{\theta}}_{F_\beta}^{\mathrm{T}}(0)\tilde{\boldsymbol{\theta}}_{F_\beta}(0) + \eta^2 \int_0^{t_f} d^{\mathrm{T}}(t)d(t)dt\end{aligned} \tag{38}$$

The inequality in Eq. (24) is satisfied for the H_∞ tracking performance. Proof 1 is proven with the above process.

Even though the stability of the IT2-NNFAC closed-loop system is assured, the update laws of Eqs. (28) and (29) cannot guarantee that the parameters $\hat{\boldsymbol{\theta}}_{F_\alpha}$ and $\hat{\boldsymbol{\theta}}_{F_\beta}$ are within the desired bounded values. Thus, it is necessary to modify the update laws using the projection algorithm for ensuring that the parameters $\hat{\boldsymbol{\theta}}_{F_\alpha}$ and $\hat{\boldsymbol{\theta}}_{F_\beta}$ are bounded for all $t \ge 0$. Let Ω_{0F_α}, Ω_{F_α}, Ω_{0F_β}, and Ω_{F_β} be as follows.

$\Omega_{0F_\alpha} = \left\{\hat{\boldsymbol{\theta}}_{F_\alpha} : \left\|\hat{\boldsymbol{\theta}}_{F_\alpha}\right\| \le \alpha_{F_\alpha}\right\}$, $\Omega_{F_\alpha} = \left\{\hat{\boldsymbol{\theta}}_{F_\alpha} : \left\|\hat{\boldsymbol{\theta}}_{F_\alpha}\right\| \le \alpha_{F_\alpha} + M_{F_\alpha}\right\}$, $\Omega_{0F_\beta} = \left\{\hat{\boldsymbol{\theta}}_{F_\beta} : \left\|\hat{\boldsymbol{\theta}}_{F_\beta}\right\| \le \alpha_{F_\beta}\right\}$, and $\Omega_{F_\beta} = \left\{\hat{\boldsymbol{\theta}}_{F_\beta} : \left\|\hat{\boldsymbol{\theta}}_{F_\beta}\right\| \le \alpha_{F_\beta} + M_{F_\beta}\right\}$, where the positive constants α_{F_α}, M_{F_α}, α_{F_β}, and M_{F_β} are specified The update law can be changed as follows according to the projection operators.

$$\dot{\hat{\boldsymbol{\theta}}}_{F_\alpha} = \begin{cases} \gamma_{F_\alpha}\boldsymbol{\xi}_{F_\alpha}(\boldsymbol{x})\mathbf{B}^{\mathrm{T}}\mathbf{P}\mathbf{e}, & \text{if } \left(\left\|\hat{\boldsymbol{\theta}}_{F_\alpha}\right\| < M_{F_\alpha}\right) \\ & \text{or } \left(\left\|\hat{\boldsymbol{\theta}}_{F_\alpha}\right\| = M_{F_\alpha} \text{ and } \hat{\boldsymbol{\theta}}_{F_\alpha}^{\mathrm{T}}\boldsymbol{\xi}_{F_\alpha}(\boldsymbol{x})\mathbf{B}^{\mathrm{T}}\mathbf{P}\mathbf{e} \le \boldsymbol{0}\right) \\ Proj\left\{\gamma_{F_\alpha}\boldsymbol{\xi}_{F_\alpha}(\boldsymbol{x})\mathbf{B}^{\mathrm{T}}\mathbf{P}\mathbf{e}\right\}, & \text{if } \left(\left\|\hat{\boldsymbol{\theta}}_{f_N}\right\| = M_{F_\alpha} \text{ and } \hat{\boldsymbol{\theta}}_{F_\alpha}^{\mathrm{T}}\boldsymbol{\xi}_{F_\alpha}(\boldsymbol{x})\mathbf{B}^{\mathrm{T}}\mathbf{P}\mathbf{e} > \boldsymbol{0}\right) \end{cases} \tag{39}$$

$$\dot{\hat{\boldsymbol{\theta}}}_{F_\beta} = \begin{cases} \gamma_{F_\beta}\boldsymbol{\xi}_{F_\beta}(\boldsymbol{x})\mathbf{B}^{\mathrm{T}}\mathbf{P}\mathbf{e}, & \text{if } \left(\left\|\hat{\boldsymbol{\theta}}_{F_\beta}\right\| < M_{F_\beta}\right) \\ & \text{or } \left(\left\|\hat{\boldsymbol{\theta}}_{F_\beta}\right\| = M_{F_\beta} \text{ and } \hat{\boldsymbol{\theta}}_{F_\beta}^{\mathrm{T}}\boldsymbol{\xi}_{F_\beta}(\boldsymbol{x})\mathbf{B}^{\mathrm{T}}\mathbf{P}\mathbf{e} \le \boldsymbol{0}\right) \\ Proj\left\{\gamma_{F_\beta}\boldsymbol{\xi}_{F_\beta}(\boldsymbol{x})\mathbf{B}^{\mathrm{T}}\mathbf{P}\mathbf{e}\right\}, & \text{if } \left(\left\|\hat{\boldsymbol{\theta}}_{F_\beta}\right\| = M_{F_\beta} \text{ and } \hat{\boldsymbol{\theta}}_{F_\beta}^{\mathrm{T}}\boldsymbol{\xi}_{F_\beta}(\boldsymbol{x})\mathbf{B}^{\mathrm{T}}\mathbf{P}\mathbf{e} > \boldsymbol{0}\right) \end{cases} \tag{40}$$

The definitions of the projection operators $Proj\left\{\gamma_{F_\alpha}\xi_{F_\alpha}(\boldsymbol{x})\mathbf{B}^{\mathrm{T}}\mathbf{Pe}\right\}$ and $Proj\left\{\gamma_{F_\beta}\xi_{F_\beta}(\boldsymbol{x})\mathbf{B}^{\mathrm{T}}\mathbf{Pe}\right\}$ are as follows.

$$Proj\left\{\gamma_{F_\alpha}\xi_{F_\alpha}(\boldsymbol{x})\mathbf{B}^{\mathrm{T}}\mathbf{Pe}\right\}=\gamma_{F_\alpha}\left(\xi_{F_\alpha}(\boldsymbol{x})\mathbf{B}^{\mathrm{T}}\mathbf{Pe}-\left(\left\|\boldsymbol{\theta}_{F_\alpha}\right\|^2-\alpha_{F_\alpha}\right)\xi_{F_\alpha}(\boldsymbol{x})\mathbf{B}^{\mathrm{T}}\mathbf{Pe}\frac{\hat{\boldsymbol{\theta}}_{F_\alpha}^{\mathrm{T}}\hat{\boldsymbol{\theta}}_{F_\alpha}}{M_{F_\alpha}\left\|\hat{\boldsymbol{\theta}}_{F_\alpha}\right\|^2}\right) \tag{41}$$

$$Proj\left\{\gamma_{F_\beta}\xi_{F_\beta}(\boldsymbol{x})\mathbf{B}^{\mathrm{T}}\mathbf{Pe}\right\}=\gamma_{F_\beta}\left(\xi_{F_\beta}(\boldsymbol{x})\mathbf{B}^{\mathrm{T}}\mathbf{Pe}-\left(\left\|\boldsymbol{\theta}_{F_\beta}\right\|^2-\alpha_{F_\beta}\right)\xi_{F_\beta}(\boldsymbol{x})\mathbf{B}^{\mathrm{T}}\mathbf{Pe}\frac{\hat{\boldsymbol{\theta}}_{F_\beta}^{\mathrm{T}}\hat{\boldsymbol{\theta}}_{F_\beta}}{M_{F_\beta}\left\|\hat{\boldsymbol{\theta}}_{F_\beta}\right\|^2}\right) \tag{42}$$

$\hat{\boldsymbol{\theta}}_{F_\alpha}^{\mathrm{T}}\hat{\boldsymbol{\theta}}_{F_\alpha}\le\alpha_{F_\alpha}+M_{F_\alpha}$ and $\hat{\boldsymbol{\theta}}_{F_\beta}^{\mathrm{T}}\hat{\boldsymbol{\theta}}_{F_\beta}\le\alpha_{F_\beta}+M_{F_\beta}$ are obtained from the constraint sets Ω_{F_α} and Ω_{F_β}. As a result, the values of α_{F_α}, M_{F_α}, α_{F_β}, and M_{F_β} (>0) are chosen randomly.

Since each $\xi_{F_\alpha}^{\ell^{\mathrm{T}}}(x),\xi_{F_\beta}^{\ell^{\mathrm{T}}}(x)\in(0,1]$ and $\sum_{\ell=1}^{p}\xi_{F_\alpha}^{\ell^{\mathrm{T}}}(\boldsymbol{x})=\sum_{\ell=1}^{p}\xi_{F_\beta}^{\ell^{\mathrm{T}}}(\boldsymbol{x})=1$, $F_\alpha(\boldsymbol{x})F_\alpha(\boldsymbol{x})\le\sigma_{F_\alpha}$ and $F_\beta(\boldsymbol{x})F_\beta(\boldsymbol{x})\le\sigma_{F_\beta}$, where $\sigma_{F_\alpha}\equiv\max_{1\le\ell\le p}(a_{F_\alpha}^{\ell}+M_{F_\alpha})$ and $\sigma_{F_\beta}\equiv\max_{1\le\ell\le p}(a_{F_\beta}^{\ell}+M_{F_\beta})$.

$$\begin{aligned}F_\alpha(\boldsymbol{x})F_\alpha(\boldsymbol{x})&\le\sum_{\ell=1}^{p}\sqrt{(a_{F_\alpha}^{\ell}+M_{F_\alpha})}\xi_{F_\alpha}^{\ell^{\mathrm{T}}}(\boldsymbol{x})\sum_{\ell=1}^{p}\sqrt{(a_{F_\alpha}^{\ell}+M_{F_\alpha})}\xi_{F_\alpha}^{\ell^{\mathrm{T}}}(\boldsymbol{x})\\&\le\sqrt{\sigma_{F_\alpha}}\sum_{\ell=1}^{p}\xi_{F_\alpha}^{\ell^{\mathrm{T}}}(\boldsymbol{x})\sqrt{\sigma_{F_\alpha}}\sum_{\ell=1}^{p}\xi_{F_\alpha}^{\ell^{\mathrm{T}}}(\boldsymbol{x})\le\sigma_{F_\alpha}\end{aligned} \tag{43}$$

$$\begin{aligned}F_\beta(\boldsymbol{x})F_\beta(\boldsymbol{x})&\le\sum_{\ell=1}^{p}\sqrt{(a_{F_\beta}^{\ell}+M_{F_\beta})}\xi_{F_\beta}^{\ell^{\mathrm{T}}}(\boldsymbol{x})\sum_{\ell=1}^{p}\sqrt{(a_{F_\beta}^{\ell}+M_{F_\beta})}\xi_{F_\beta}^{\ell^{\mathrm{T}}}(\boldsymbol{x})\\&\le\sqrt{\sigma_{F_\beta}}\sum_{\ell=1}^{p}\xi_{F_\beta}^{\ell^{\mathrm{T}}}(\boldsymbol{x})\sqrt{\sigma_{F_\beta}}\sum_{\ell=1}^{p}\xi_{F_\beta}^{\ell^{\mathrm{T}}}(\boldsymbol{x})\le\sigma_{F_\beta}\end{aligned} \tag{44}$$

Therefore, the sets are simplified as $\hat{\boldsymbol{\theta}}_{F_\alpha}^{\mathrm{T}}\hat{\boldsymbol{\theta}}_{F_\alpha}\le\sigma_{F_\alpha}$ and $\hat{\boldsymbol{\theta}}_{F_\beta}^{\mathrm{T}}\hat{\boldsymbol{\theta}}_{F_\beta}\le\sigma_{F_\beta}$, where $\sigma_{F_\alpha}=\max\left(\hat{\theta}_{F_\alpha}^{\mathrm{T}}\hat{\theta}_{F_\alpha}\right)$ and $\sigma_{F_\beta}=\max\left(\hat{\boldsymbol{\theta}}_{F_\beta}^{\mathrm{T}}\hat{\boldsymbol{\theta}}_{F_\beta}\right)$. As a result, it is possible to guarantee the stability of the system when using projection operators.

3.2.1.1 Remark 1

The attenuation level η is required to satisfy the following inequality from the Riccati equation in Theorem 2 [Eq. (27)].

$$-\frac{2}{\gamma} + \frac{1}{\eta^2} \leq 0 \text{ or } \gamma \leq 2\eta^2 \tag{45}$$

To achieve H_∞ tracking performance, the estimation and tracking errors of the SISO nonlinear system must be minimized in terms of disturbance.

3.2.1.2 Remark 2

A saturation function is replaced with sgn($\mathbf{B}^T\mathbf{Pe}$) because the control law provided by Eq. (26) containing sgn($\mathbf{B}^T\mathbf{Pe}$) results in chattering effects.[35]

$$sat(\mathbf{B}^T\mathbf{Pe}) = \begin{cases} \text{sgn}(\mathbf{B}^T\mathbf{Pe}/\lambda), & \text{if } \left\|\mathbf{B}^T\mathbf{Pe}\right\| \geq \lambda \\ \mathbf{B}^T\mathbf{Pe}/\lambda, & \text{if } \left\|\mathbf{B}^T\mathbf{Pe}\right\| \leq \lambda \end{cases} \tag{46}$$

Here, λ is a positive constant.

3.2.1.3 Theorem 3

Sectorial dead zone nonlinearities $\Phi(u)$ and uncertain nonlinear functions $F_\alpha(x)$ and $F_\beta(x)$ in a controlled system are expressed as IT2NNFAC equations using Eqs. (21), (25), and (26). Here, $\boldsymbol{P} = \boldsymbol{P}^T > 0$ satisfies Eq. (27) at a prescribed attenuation level $0 < \eta < 1$. Equations (39) and (40) are then selected as the updated law. Following that, for any bounded value of $\boldsymbol{e}$, $\tilde{\boldsymbol{\theta}}_{F_\alpha}$, and $\tilde{\boldsymbol{\theta}}_{F_\beta}$ at $t \geq 0$, H_∞ tracking performance is achieved within a predetermined value η^2 in the presence of external disturbances.

3.2.2 Proof 2

From the candidate of Lyapunov function [Eq. (30)] and $\dot{\tilde{\boldsymbol{\theta}}}_{F_\alpha} = \dot{\hat{\boldsymbol{\theta}}}_{F_\alpha}$ and $\dot{\tilde{\boldsymbol{\theta}}}_{F_\beta} = \dot{\hat{\boldsymbol{\theta}}}_{F_\beta}$, Proof 1 is applied to Theorem 2; then, the following is obtained.

$$\begin{aligned}\dot{V}=&\frac{1}{2}\mathbf{e}^{\mathrm{T}}\left(\mathbf{A}_m^{\mathrm{T}}\mathbf{P}+\mathbf{P}\mathbf{A}_m+\left(-\frac{2}{\gamma}+\frac{1}{\eta^2}\right)\mathbf{P}\mathbf{B}\mathbf{B}^{\mathrm{T}}\mathbf{P}\right)\mathbf{e}+\frac{1}{2}\eta^2 d^{\mathrm{T}}d\\&-\frac{1}{2}\left(\frac{1}{\eta}\mathbf{B}^{\mathrm{T}}\mathbf{P}\mathbf{e}-\eta d\right)^{\mathrm{T}}\left(\frac{1}{\eta}\mathbf{B}^{\mathrm{T}}\mathbf{P}\mathbf{e}-\eta d\right)\\&+\mathbf{e}^{\mathrm{T}}\mathbf{P}\mathbf{B}\left(-\boldsymbol{\xi}_{F_\alpha}^{\mathrm{T}}(\boldsymbol{x})\tilde{\boldsymbol{\theta}}_{F_\alpha}-\boldsymbol{\xi}_{F_\beta}^{\mathrm{T}}(\boldsymbol{x})\tilde{\boldsymbol{\theta}}_{F_\beta}+\tilde{F}_\alpha+\tilde{F}_\beta+u_\varepsilon\right)\\&+\frac{1}{\gamma_{F_\alpha}}\tilde{\boldsymbol{\theta}}_{F_\alpha}^{\mathrm{T}}\dot{\tilde{\boldsymbol{\theta}}}_{F_\alpha}+\frac{1}{\gamma_{F_\beta}}\tilde{\boldsymbol{\theta}}_{F_\beta}^{\mathrm{T}}\dot{\tilde{\boldsymbol{\theta}}}_{F_\beta}\end{aligned}\tag{47}$$

By using the adaptive laws of Eqs. (39) and (40) and applying the Riccati inequality [Eq. (27)], Eq. (47) is transformed to

$$\begin{aligned}\dot{V}\le&-\frac{1}{2}\mathbf{e}^{\mathrm{T}}\mathbf{Q}\mathbf{e}+\frac{1}{2}\eta^2 d^{\mathrm{T}}d\\&+\frac{1}{\gamma_{f_N}}\tilde{\boldsymbol{\theta}}_{F_\alpha}^{\mathrm{T}}\gamma_{F_\alpha}\left(\boldsymbol{\xi}_{F_\alpha}(\boldsymbol{x})\mathbf{B}^{\mathrm{T}}\mathbf{P}\mathbf{e}-\left(\left\|\boldsymbol{\theta}_{F_\alpha}\right\|^2-\alpha_{F_\alpha}\right)\boldsymbol{\xi}_{F_\alpha}(\boldsymbol{x})\mathbf{B}^{\mathrm{T}}\mathbf{P}\mathbf{e}\frac{\hat{\boldsymbol{\theta}}_{F_\alpha}^{\mathrm{T}}\hat{\boldsymbol{\theta}}_{F_\alpha}}{M_{F_\alpha}\left\|\hat{\boldsymbol{\theta}}_{F_\alpha}\right\|^2}\right)\\&+\frac{1}{\gamma_{F_\beta}}\tilde{\boldsymbol{\theta}}_{F_\beta}^{\mathrm{T}}\gamma_{F_\beta}\left(\boldsymbol{\xi}_{F_\beta}(\boldsymbol{x})\mathbf{B}^{\mathrm{T}}\mathbf{P}\mathbf{e}-\left(\left\|\boldsymbol{\theta}_{F_\beta}\right\|^2-\alpha_{F_\beta}\right)\boldsymbol{\xi}_{F_\beta}(\boldsymbol{x})\mathbf{B}^{\mathrm{T}}\mathbf{P}\mathbf{e}\frac{\hat{\boldsymbol{\theta}}_{F_\beta}^{\mathrm{T}}\hat{\boldsymbol{\theta}}_{F_\beta}}{M_{F_\beta}\left\|\hat{\boldsymbol{\theta}}_{F_\beta}\right\|^2}\right)\\&-\tilde{\boldsymbol{\theta}}_{F_\alpha}^{\mathrm{T}}\boldsymbol{\xi}_{F_\alpha}(\boldsymbol{x})\mathbf{B}^{\mathrm{T}}\mathbf{P}\mathbf{e}-\tilde{\boldsymbol{\theta}}_{F_\beta}^{\mathrm{T}}\boldsymbol{\xi}_{F_\beta}(\boldsymbol{x})\mathbf{B}^{\mathrm{T}}\mathbf{P}\mathbf{e}+\mathbf{e}^{\mathrm{T}}\mathbf{P}\mathbf{B}\left(\tilde{F}_\alpha+\tilde{F}_\beta\right)+\mathbf{e}^{\mathrm{T}}\mathbf{P}\mathbf{B}u_\varepsilon\end{aligned}\tag{48}$$

Then, substituting Eq. (46) with Eq. (48) yields

$$\begin{aligned}\dot{V}&\le-\frac{1}{2}\mathbf{e}^{\mathrm{T}}\mathbf{Q}\mathbf{e}+\frac{1}{2}\eta^2 d^{\mathrm{T}}d+\mathbf{e}^{\mathrm{T}}\mathbf{P}\mathbf{B}\left(\tilde{F}_\alpha+\tilde{F}_\beta\right)-\mathbf{e}^{\mathrm{T}}\mathbf{P}\mathbf{B}M_e(\boldsymbol{x})sat(\mathbf{B}^{\mathrm{T}}\mathbf{P}\mathbf{e})\\&\le-\frac{1}{2}\mathbf{e}^{\mathrm{T}}\mathbf{Q}\mathbf{e}+\frac{1}{2}\eta^2 d^{\mathrm{T}}d+M_e(\boldsymbol{x})\left\|\mathbf{e}^{\mathrm{T}}\mathbf{P}\mathbf{B}\right\|-M_e(\boldsymbol{x})\left\|\mathbf{e}^{\mathrm{T}}\mathbf{P}\mathbf{B}\right\|\\&\le-\frac{1}{2}\mathbf{e}^{\mathrm{T}}\mathbf{Q}\mathbf{e}+\frac{1}{2}\eta^2 d^{\mathrm{T}}d\end{aligned}\tag{49}$$

Therefore,

$$\|\boldsymbol{e}\|\ge\frac{\eta\sqrt{d^{\mathrm{T}}d}}{\lambda_{min}(\boldsymbol{Q})}\tag{50}$$

With respect to $\dot{V} \le 0$, $\lambda_{min}(\mathbf{Q})$ stands for the minimal eigenvalue of $\mathbf{Q}$. The retarded functional differential equation is examined under the Lyapunov stability theory.[33,37] All uncertainties are guaranteed to be within the boundary of $\mathbf{e}$ and x_m, as well as the parameter estimation errors $\tilde{\boldsymbol{\theta}}_{F_\alpha}$ and $\tilde{\boldsymbol{\theta}}_{F_\beta}$, since η is the designed constant acting as an attenuation level.[34] Equations (35) and (36) from $t = 0$ to $t = t_f$ are integrated for $t \ge 0$, which produces the following.

$$2V(t_f) - 2V(0) \le -\int_0^{t_f} \mathbf{e}^{\mathrm{T}}(t)\mathbf{Q}\mathbf{e}(t)dt + \eta^2 \int_0^{t_f} d^{\mathrm{T}}(t)d(t)dt \tag{51}$$

Since $V(t_f) \ge 0$, the inequality of Eq. (51) produces

$$\begin{aligned}\int_0^{t_f} \mathbf{e}^T(t)\mathbf{Q}\mathbf{e}(t)dt \le 2\mathbf{e}^T(0)\mathbf{P}\mathbf{e}(0) &+ \frac{2}{\gamma_{F_\alpha}}\tilde{\boldsymbol{\theta}}_{F_\alpha}^T(0)\tilde{\boldsymbol{\theta}}_{F_\alpha}(0) \\ &+ \frac{2}{\gamma_{F_\beta}}\tilde{\boldsymbol{\theta}}_{F_\beta}^T(0)\tilde{\boldsymbol{\theta}}_{F_\beta}(0) + \eta^2 \int_0^{t_f} d^T(t)d(t)dt\end{aligned} \tag{52}$$

With the H_∞ tracking performance, the inequality [Eq. (24)] is satisfied. Therefore, Proof 2 is proven. The overall design of the proposed IT2NNFAC is shown in Fig. 6. The following is a description of the design process for IT2NNFAC with H_∞ tracking performance.

Step 1: The values of $\alpha_{F_\alpha}^{\ell}$, M_{F_α}, $\alpha_{F_\beta}^{\ell}$, and M_{F_β} are determined based on $F_{\alpha_{max}}$, $F_{\alpha_{\min}}$, $F_{\beta_{max}}$, and $F_{\beta_{\min}}$ and the parameters of α, ε, ε^-, ε^+, κ, $\underline{\kappa}$, $\overline{\kappa}$, γ_{F_α}, γ_{F_β}, α_{F_α}, M_{F_α}, α_{F_β}, M_{F_β}, M_e at the initial conditions of x, $\boldsymbol{\theta}_{F_\alpha}$, and $\boldsymbol{\theta}_{F_\beta}$. Here, $l = 1, 2, ..., p$, and p is a number defined by fuzzy rules.

Step 2: The feedback gain $\mathbf{k}$ is set so that all of the roots of the $\mathbf{A_m} = \mathbf{A} - \mathbf{B}\mathbf{k}^T$-characteristic polynomials have negative real parts.

Step 3: Defining $\mu_{F_{F_{\alpha i}}^{\ell}}(x_i)$, $\mu_{F_{F_{\beta i}}^{\ell}}(x_i)$, $i = 1, 2, ..., n$, $l = 1, 2, ..., p$, membership functions for state variables x are found in the controlled system.

Step 4: Selecting the values γ and η and the weighting matrix $\mathbf{Q}$ allows the positive definite symmetric matrix $\mathbf{P}$ as a solution to the Riccati equation [Eq. (27)]. A new $\mathbf{Q}$ is selected to solve Eq. (27) if there is no positive definite symmetric matrix $\mathbf{P}$.

Step 5: By applying Eqs. (25) and (26) to the controlled system, IT2NNFAC is obtained with tracking performance [Eq. (21)].

Step 6: $\boldsymbol{\theta}_{F_\alpha}$ and $\boldsymbol{\theta}_{F_\beta}$ are adjusted by computing the update laws [Eqs. (28) and (29)].

These steps are repeated to control the nonlinear system with IT2NNFAC with H_∞ tracking performance.

3.2.2.1 Remark 3

The value of η is reduced to decrease disturbances and sectorial dead zone nonlinearities if the output is unsatisfactory. Additionally, the upper boundary of the steady-state errors $\mathbf{e}(t)$ decreases as η is sufficiently increased.

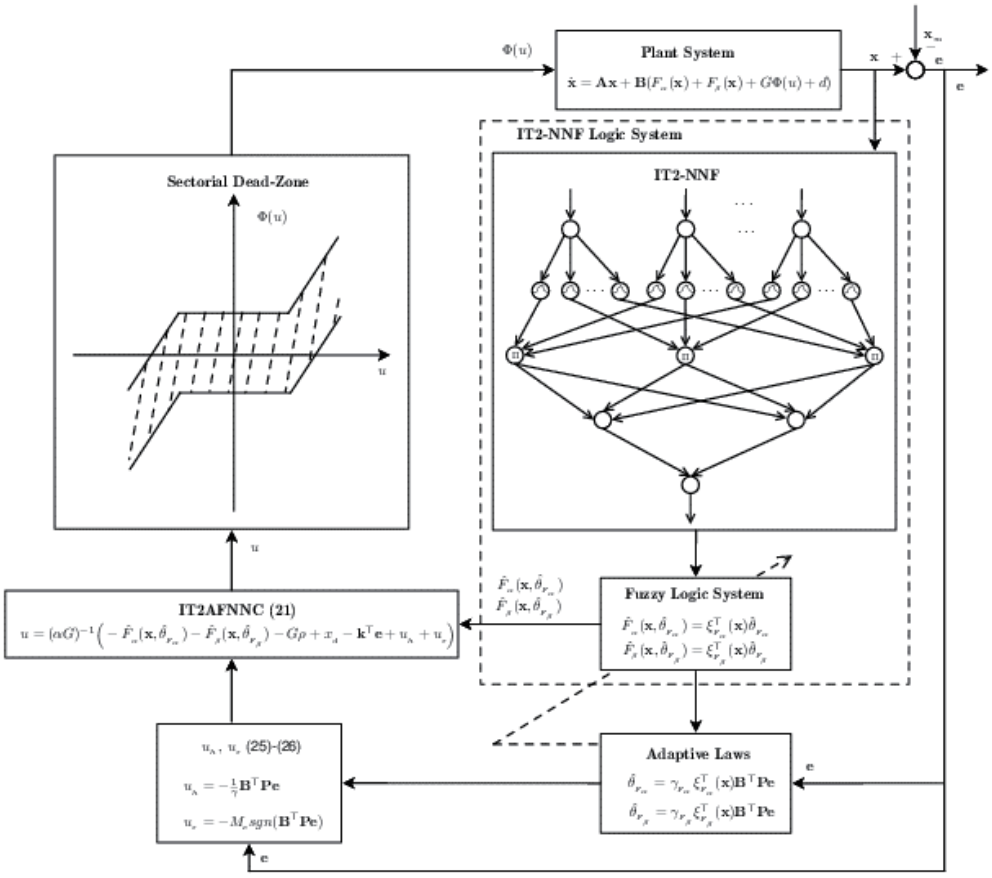

Fig. 6. Overall scheme of proposed ITNNFAC.

4. Results of Simulation

As shown in Fig. 7, a mass spring damper system[38] is simulated using the proposed IT2NNFAC in the presence of ambiguous parameters and exogenous disturbances.

4.1 Mass spring damper system

The associated mathematical model is explained as follows.

$$\begin{cases} \dot{x}_1 = x_2 \\ \dot{x}_2 = \dfrac{-F_\alpha(x,t) - F_\beta(x,t) + G\Phi(u)}{M} + d(x,t) \end{cases} \tag{53}$$

Here, $y = x_1$ represents the displacement of the mass, x_2 represents its velocity, $F_a(x,t) = {x_1}^2$ represents the spring force, $F_a(x,t) = 0.5{x_2}^3$ represents the friction force, $M = 0.75$ kg represents the body mass, $u(t)$ represents the applied force, and $G = 1$. It is assumed that the exogenous

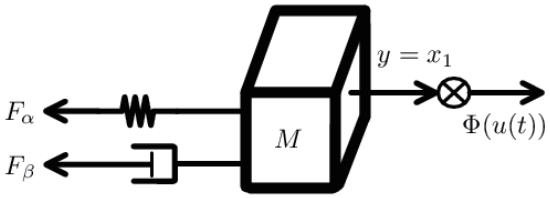

Fig. 7. Mass spring damper system simulation using proposed IT2NNFAC.

disturbance is $d(x,t) = 0.1x_2\sin(t)$, and assumed to be unknown are the structures of the spring and friction forces.

4.2 Simulation process

IT2NNFAC in Eq. (21) is performed following the process above as follows.

4.2.1 Step 1

First, the parameters of the sectorial dead zone nonlinearities for the mass spring damper system are defined as $\varepsilon_1^+ = 0.99$, $\varepsilon_1^- = -0.99$, $\varepsilon_2^+ = 0.1$, $\varepsilon_1^- = -0.1$, $\overline{\kappa}_1 = 0.99$, $\underline{\kappa}_1 = -0.99$, $\overline{\kappa}_2 = 0.1$, $\underline{\kappa}_2 = -0.1$, and $\alpha = \alpha' = \underline{\alpha} = \overline{\alpha} = 1$. Then, the boundary is selected as $\alpha_{max} = 1.55$, $\alpha_{min} = 0.65$, $\varepsilon_{1imax}^+ = \varepsilon_{2imax}^+ = \overline{\kappa}_{1imax} = \overline{\kappa}_{2imax} = 1$, $\varepsilon_{1imin}^- = \varepsilon_{2imin}^- = \underline{\kappa}_{1imin} = \underline{\kappa}_{2imin} = -1$, and

$$\rho_1 = max\left\{\left|\alpha_{max}\varepsilon_{1imax}^+ + \overline{\kappa}_{1imax}\right|, \left|\alpha_{min}\varepsilon_{1imin}^- + \underline{\kappa}_{1imin}\right|\right\} = 2.25 \tag{54}$$

$$\rho_2 = max\left\{\left|\alpha_{max}\varepsilon_{2imax}^+ + \overline{\kappa}_{2imax}\right|, \left|\alpha_{min}\varepsilon_{2imin}^- + \underline{\kappa}_{2imin}\right|\right\} = 2.25 \tag{55}$$

4.2.2 Step 2

The simulation is set up with three fuzzy rules. Figure 5 shows the Gaussian membership function. To reduce the effect of the estimated velocity, fuzzy rules are built on the basis of mass displacement and mass velocity inaccuracies. The borders are determined using the boundary conditions of the system: $F_{\alpha_{max}} = 2.1329$, $F_{\alpha_{min}} = -1.9622$, $F_{\beta_{max}} = 2.3929$, and $F_{\beta_{min}} = 0$. As a result, $\alpha_{F_\alpha} = 150$, $\alpha_{F_\beta} = 750$, and $M_{F_\alpha} = 350$, $M_{F_\beta} = 850$ are selected as the values of the constraint regions Ω_{F_α} and Ω_{F_β}. The initial values $\boldsymbol{\theta}_{F_\alpha}(0)$ and $\boldsymbol{\theta}_{F_\beta}(0)$ are then set to $\boldsymbol{\theta}_{F_\alpha}(0) = 0.65\mathrm{I}_{50\times1}$ and $\boldsymbol{\theta}_{F_\beta}(0) = 1.75\mathrm{I}_{50\times1}$, which are selected from $F_{\alpha_{max}}$, $F_{\alpha_{min}}$ ($F_{\alpha_{min}} \le \theta_{F_\alpha}(0) \le F_{\alpha_{max}}$) and $F_{\beta_{max}}$, $F_{\beta_{min}}$ ($F_{\beta_{min}} \le \theta_{F_\beta}(0) \le F_{\beta_{max}}$), respectively. The design parameters are selected as $\gamma_{F_\alpha} = 0.5$, $\gamma_{F_\beta} = 0.1$, and the sampling time $h = 0.01$. The boundary of the uncertainty $M_e = 3.51$. The initial conditions are chosen to be $\boldsymbol{x}(0) = \left[x_1(0)\ \ x_2(0)\right]^T = \left[2.1\ \ -2.1\right]^T$, where x_1 and x_2 follow the reference trajectories $\boldsymbol{x}_m = \left[x_{m_1}(0)\ \ x_{m_2}(0)\right]^T = \left[2\sin(t)\ \ 2\cos(t)\right]^T$.

4.2.3 Step 3

The feedback gain $\mathbf{k}^{\mathrm{T}} = \begin{bmatrix} -20 & -45 \\ -35 & 75 \end{bmatrix}$ is set so that all of the roots of $\mathbf{A}_{\mathrm{m}} = \mathbf{A} - \mathbf{B}\mathbf{k}^{\mathrm{T}}$, which are characteristic polynomials, have negative real parts. The values $\gamma = 0.55$ and $\eta = 0.5$ and the weighting matrix $\mathbf{Q} = 0.0061\ \mathrm{I}_{2\times 2}$ are selected to obtain the positive definite symmetric matrix **P** as the solution to the Riccati equation. As a result, the matrix **P** is determined as Eq. (56).

$$\mathbf{P} = \begin{bmatrix} 6.1805 & 0.2495 \\ 0.2495 & 0.2823 \end{bmatrix} \tag{56}$$

4.2.4 Step 4

To approximate $F_\alpha(x)$ and $F_\beta(x)$, which are unknown nonlinear functions, the upper and lower boundaries of the membership functions (Fig. 5) are expressed in the forms of $\overline{\mu}_{C^{\ell}_{F_\alpha}}\left(\hat{y}_{F_\alpha}\right)$, $\overline{\mu}_{C^{\ell}_{F_\beta}}\left(\hat{y}_{F_\beta}\right)$, $\underline{\mu}_{C^{\ell}_{F_\alpha}}\left(\hat{y}_{F_\alpha}\right)$, and $\underline{\mu}_{C^{\ell}_{F_\beta}}\left(\hat{y}_{F_\beta}\right)$. The mathematical means of the defuzzified output are $F^{\ell}_{\alpha} = \frac{1}{2}\left(\overline{F}^{\ell}_{\alpha} + \underline{F}^{\ell}_{\alpha}\right)$ and $F^{\ell}_{\beta} = \frac{1}{2}\left(\overline{F}^{\ell}_{\beta} + \underline{F}^{\ell}_{\beta}\right)$. Thus, the Gaussian membership functions of IT2NNF for x_i (i = 1, 2) (Fig. 5) are expressed as follows.

$$\overline{\mu}_{F^{\ell}_{F_{\alpha 1}}}\left(x_1\right) = e^{-\left(\frac{x_1+\pi/6}{\pi/18}\right)^2},\ \overline{\mu}_{F^{\ell}_{F_{\alpha 2}}}\left(x_1\right) = e^{-\left(\frac{x_1}{\pi/18}\right)^2},\ \overline{\mu}_{F^{\ell}_{F_{\alpha 3}}}\left(x_1\right) = e^{-\left(\frac{x_1-\pi/6}{\pi/18}\right)^2} \tag{57}$$

$$\overline{\mu}_{F^{\ell}_{F_{\beta 1}}}\left(x_1\right) = e^{-\left(\frac{x_1+\pi/6}{\pi/18}\right)^2},\ \overline{\mu}_{F^{\ell}_{F_{\beta 2}}}\left(x_1\right) = e^{-\left(\frac{x_1}{\pi/18}\right)^2},\ \overline{\mu}_{F^{\ell}_{F_{\beta 3}}}\left(x_1\right) = e^{-\left(\frac{x_1-\pi/6}{\pi/18}\right)^2} \tag{58}$$

$$\underline{\mu}_{F^{\ell}_{F_{\alpha 1}}}\left(x_1\right) = a_{F_{\alpha 1}} e^{-\left(\frac{x_1+\pi/6}{\pi/24}\right)^2},\ \underline{\mu}_{F^{\ell}_{F_{\alpha 2}}}\left(x_1\right) = a_{F_{\alpha 2}} e^{-\left(\frac{x_1}{\pi/24}\right)^2},\ \underline{\mu}_{F^{\ell}_{F_{\alpha 3}}}\left(x_1\right) = a_{F_{\alpha 3}} e^{-\left(\frac{x_1-\pi/6}{\pi/24}\right)^2} \tag{59}$$

$$\underline{\mu}_{F^{\ell}_{F_{\beta 1}}}\left(x_1\right) = a_{F_{\beta 1}} e^{-\left(\frac{x_1+\pi/6}{\pi/24}\right)^2},\ \underline{\mu}_{F^{\ell}_{F_{\beta 2}}}\left(x_1\right) = a_{F_{\beta 2}} e^{-\left(\frac{x_1}{\pi/24}\right)^2},\ \underline{\mu}_{F^{\ell}_{F_{\beta 3}}}\left(x_1\right) = a_{F_{\beta 3}} e^{-\left(\frac{x_1-\pi/6}{\pi/24}\right)^2} \tag{60}$$

where $a_{F_{\alpha 1}} = a_{F_{\alpha 2}} = a_{F_{\alpha 3}} = 0.25$ and $a_{F_{\beta 1}} = a_{F_{\beta 2}} = a_{F_{\beta 3}} = 0.85$.

With the use of the singleton fuzzifier and product inference,

$$\overline{F}^{\ell}_{F_\alpha} = 1 \times \Pi^{2}_{p=1} \overline{\mu}_{F^{\ell}_{F_{\alpha p}}}\left(x_p\right),\ \underline{F}^{\ell}_{F_\alpha} = b_{F_\alpha} \times \Pi^{2}_{p=1} \underline{\mu}_{F^{\ell}_{F_{\alpha p}}}\left(x_p\right) \tag{61}$$

$$\overline{F}^{\ell}_{F_\beta} = 1 \times \Pi^{2}_{p=1} \overline{\mu}_{F^{\ell}_{F_{\beta_p}}}\left(x_p\right),\ \underline{F}^{\ell}_{F_\beta} = b_{F_\beta} \times \Pi^{2}_{p=1} \underline{\mu}_{F^{\ell}_{F_{\beta_p}}}\left(x_p\right) \tag{62}$$

where $b_{F_\alpha} = 0.34$ and $b_{F_\beta} = 0.22$.

4.2.5 Step 5

The mass spring damper system is subjected to the control force in Eq. (21). The parameter vectors $\theta_{F_\alpha}(0)$ and $\theta_{F_\beta}(0)$ are then adjusted using the update laws [Eqs. (39) and (40)]. Step 5 is repeated to apply the controller [Eq. (21)] and control the mass spring damper system.

4.3 Simulation results

The simulation results of the mass spring damper system for the proposed IT2NNFAC with H_∞ tracking performances with η = 0.05 are shown in Figs. 8–12. Figures 8 and 9 show the reactions of the displacement of mass x_1 and the velocity of mass x_2, whereas Figs. 10 and 11 present the tracking errors for e_1 and e_2, respectively. Figure 12 shows the control input u. The intended reference input functions $x_{m_1} = 2\sin(t)$ and $x_{m_2} = 2\cos(t)$ and their trajectories are shown in Figs. 8 and 9 at η = 0.05 in 2.5 s.

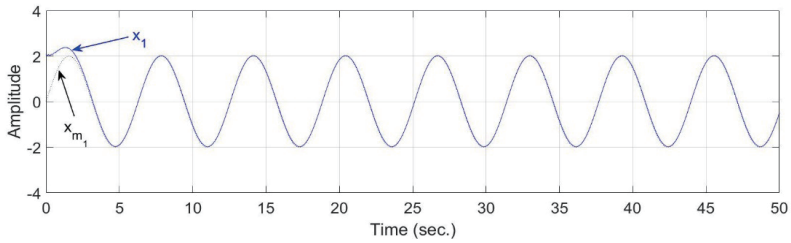

Fig. 8. (Color online) Trajectories of states $x_1(t)$ and $x_{mi}(t)$ with dead zone nonlinearities at attenuation level η = 0.5.

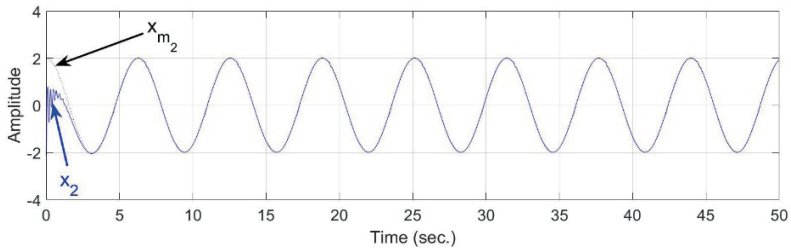

Fig. 9. (Color online) Trajectories of the states $x_2(t)$ and $x_{m2}(t)$ with dead zone nonlinearities at attenuation level η = 0.5.

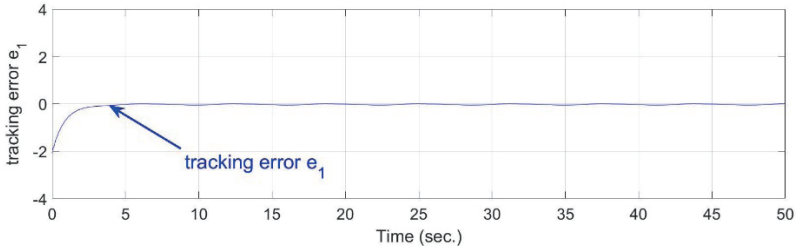

Fig. 10. (Color online) Trajectories of tracking error $e_1(t)$ with dead zone nonlinearities at attenuation level η = 0.5.

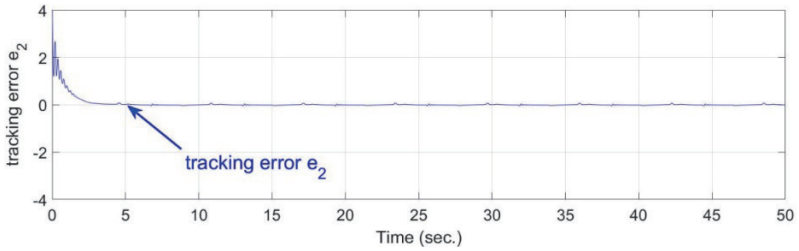

Fig. 11. (Color online) Trajectories of tracking error $e_2(t)$ with dead zone nonlinearities at attenuation level $\eta = 0.5$.

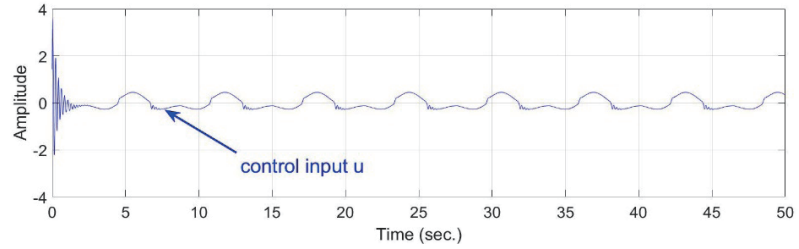

Fig. 12. (Color online) Trajectories of control input u with dead zone nonlinearities at attenuation level $\eta = 0.5$.

The following performance indices are used to demonstrate the viability and efficacy of the proposed IT2NNFAC for H_∞ tracking performance.

$$SAE = \sum \left| x_{m_p}(t) - x_p(t) \right|, \text{ for } p=1,2 \tag{63}$$

$$STAE = \sum t \left| x_{m_p}(t) - x_p(t) \right|, \text{ for } p=1,2 \tag{64}$$

$$SSE = \sum (x_{m_p}(t) - x_p(t))^2, \text{ for } p=1,2 \tag{65}$$

$$STSE = \sum t(x_{m_p}(t) - x_p(t))^2, \text{ for } p=1,2 \tag{66}$$

$$MSE = \sum \frac{1}{t} \left(x_{m_p}(t) - x_p(t) \right)^2, \text{ for } p=1,2 \tag{67}$$

$$SAC = \sum \left| u_i(t) \right| \tag{68}$$

Here, t represents a duration between 0 and 50 s, **s** represents a sample rate, SAE, STAE, SSE, STSE, MSE, and SAC are the sum of the absolute errors, the sum of the time absolute errors, the sum of the square errors, the sum of the time square errors, the mean square errors, and the sum of the absolute controller, respectively. Table 1 provides an overview of the performance indices [Eqs. (63)–(68)] for the mass spring damper system with sectorial dead zone nonlinearities at the

Table 1
Performance comparisons for performance indices [Eqs. (63)–(68)] at attenuation level $\eta = 0.5$.

Performance indices	Value	Performance indices	Value
SAE for e_1	319.5537	SAE for e_2	207.0957
STAE for e_1	10.130×10^3	STAE for e_2	11.223×10^3
SSE for e_1	44.654×10^3	SSE for e_2	40.711×10^3
STSE for e_1	2100.86×10^3	STSE for e_2	2100.4×10^3
MSE for e_1	864.230	MSE for e_2	774.5327
		SAC for u	99.3458

required attenuation level $\eta = 0.05$. When there are external disturbances and the system approaches the steady state, the performance is improved.

5. Conclusions

The sectorial dead zone nonlinearities are the major problems in diverse industrial processes and limit the performance of the manufacturing systems. Therefore, various fuzzy control systems have been proposed to solve the problems based on ANNs and FLSs. The consequences of nonlinearities are diminished in a nonlinear system with adequate mathematical models by fuzzy control using heuristic knowledge or linguistic information. With the integration of ANN and FLS, T1FNN and T2FNN have been proposed as they simplify the computational process of T1FNN and allow the fuzzy process in a multilayer interval neural network. To achieve H_∞ tracking performance with dead zone nonlinearities, IT2NNFAC is developed in this study. As the mass spring damper system requires a solution for dead zone nonlinearities for high-precision movements, a simulation for the mass spring damper system is performed to validate the performance of the proposed IT2NNFAC using online update laws and fuzzy inference based on the Lyapunov stability criterion and Riccati inequality. The result shows that IT2NNFAC stabilizes the closed-loop system by reducing external disturbances and tracking errors at any level. By using fuzzy set membership functions instead of the SISO nonlinear system function, the proposed IT2NNFAC eliminates the uncertainty resulting from unknown system parameters. The tracking errors from fuzzy approximation errors are also reduced significantly with satisfactory H_∞ tracking performance. As a result, the mass spring damper system can have faster tracking responses for sectorial dead zone, nonlinearities, and external disturbances. The proposed IT2NNFAC can provide an effective way to estimate the effect of dead zone nonlinearities on the operation of various mechanical components as well as the design of sensors and the process of sensor data to improve the performance of machinery.

Acknowledgments

The authors would like to thank the associate editor and reviewers for their valuable comments.

References

1 Z. Wei and Y. Ma: Inform. Sci. **566** (2021) 239. https://doi.org/10.1016/j.ins.2021.02.073
2 X. You, M. Shi, B. Guo, Y. Zhu, W. Lai, S. Dian, and K. Liu: Chaos Solitons Fractals (2022). https://doi.org/10.1016/j.chaos.2022.112393
3 Y. Yan, T. Li, H. Yang, J. Wang, and C. L. Philip Chen: Inf. Sci. **161** (2023) 51. https://doi.org/10.1016/j.ins.2023.02.082
4 W. Su, X. Zhao, B. Niu, G. Zhang, and H. Wang: Neurocomputing **476** (2022) 137. https://doi.org/10.1016/j.neucom.2021.12.103
5 F. Guo, Q. Chu, and C. Li: Energy Rep. **9** (2023) 416. https://doi.org/10.1016/j.egyr.2023.03.015
6 S. Zhang, D. Zhang, C. Chang, Q. Fu, and Y. Wang: Neurocomputing **329** (2019) 486. https://doi.org/10.1016/j.neucom.2018.09.032
7 Y. Wang, Z. Chen, M. Sun, and Q. Sun: Inf. Sci. **626** (2023) 75. https://doi.org/10.1016/j.ins.2023.01.060
8 B. Wu, M. Chen, S. Shao, and L. Zhang: Neurocomputing **446** (2021) 23. https://doi.org/10.1016/j.neucom.2021.02.077
9 Q. Yao: Adv. Space Res. **67** (2021) 1830. https://doi.org/10.1016/j.asr.2021.01.001.
10 B. Dong, T. An, X. Zhu, Y. Li, and K. Liu: Neurocomputing **450** (2021) 183. https://doi.org/10.1016/j.neucom.2021.04.032
11 A. Bali, U. P. Singh, R. Kumar, and S. Jain: Eur. J. Control **71** (2023) 100799. https://doi.org/10.1016/j.ejcon.2023.100799
12 Z. Lu, J. Zhang, B. Xu, D. Wang, Q. Su, J. Qian, G. Yang, and M. Pan: ISA Trans. **94** (2021) 234. https://doi.org/10.1016/j.isatra.2019.03.030
13 Y. Wu, W. Niu, L. Kong, X. Yu, and W. He: ISA Trans. **135** (2023) 449. https://doi.org/10.1016/j.isatra.2022.09.030
14 A. A. Jafari, S. M. A. Mohammadi, and M. H. Naseriyeh: Appl. Math. Model. **69** (2019) 506. https://doi.org/10.1016/j.apm.2019.01.002
15 A. S. Badr: Appl. Soft Comput. **115** (2022) 108258. https://doi.org/10.1016/j.asoc.2021.108258
16 Y. Wang and Y. Ma: Inf. Sci. **623** (2023) 559. https://doi.org/10.1016/j.ins.2022.12.055
17 R. V. Aravind and P. Balasubramaniam: Inf. Sci. **589** (2022) 213. https://doi.org/10.1016/j.ins.2021.12.082
18 A. Li, M. Liu, X. Cao, and R. Liu: Inf. Sci. **587** (2022) 746. https://doi.org/10.1016/j.ins.2021.11.002
19 S. Liu, B. Niu, G. Zong, X. Zhao, and N. Xu: Appl. Math. Comput. **435** (2022) 127441. https://doi.org/10.1016/j.amc.2022.127441
20 Y. Zhou and X. Wang: Neurocomputing **493** (2022) 474. https://doi.org/10.1016/j.neucom.2021.12.091
21 S. Kang, P. X. Liu, and H. Wang: ISA Trans. **135** (2023) 476. https://doi.org/10.1016/j.isatra.2022.09.028
22 X. Sun, L. Zhang, and J. Gu: Inf. Sci. **628** (2023) 240. https://doi.org/10.1016/j.ins.2022.12.118
23 W. Tu and J. Dong: Fuzzy Sets Syst. **464** (2023) 108481. https://doi.org/10.1016/j.fss.2023.02.002
24 Z. Sun, S. Hu, H. Xie, H. Li, J. Zheng, and B. Chen: Comput. Electr. Eng. **105** (2023) 108529. https://doi.org/10.1016/j.compeleceng.2022.108529
25 X. Liu, Y. Lin, and S. P. Wan: Inf. Sci. **570** (2023) 468. https://doi.org/10.1016/j.ins.2021.04.032
26 D. Liang, Y. Wu, and W. Duan: Inf. Sci. **631** (2023) 305. https://doi.org/10.1016/j.ins.2023.02.070
27 W. S. Yu and H.S. Chen: Inf. Sci. **288** (2014) 134. https://doi.org/10.1016/j.ins.2014.07.004
28 J. Zhao, Z.. Zhong, C. M. Lin, and H. K. Lam: J. Franklin Inst. **358** (2021) 650. https://doi.org/10.1016/j.jfranklin.2020.10.047
29 A. Dass, S. Srivastava, and R. Kumar: Appl. Soft Comput. **137** (2023) 110161. https://doi.org/10.1016/j.asoc.2023.110161
30 A. Mohammadzadeh, S. Ghaemi, O. Kaynak, S. Khanmohammadi: IEEE Trans. Fuzzy Syst. **24** (2016) 1544. https://doi.org/10.1109/TFUZZ.2016.2540067
31 M. H. Demir and B. Eren: Int. J. Hydrog. Energy **47** (2022) 19837. https://doi.org/10.1016/j.ijhydene.2022.03.113
32 M. H. Haider, Z. Wang, A. A. Khan, H. Ali, H. Zheng, S. Usman, R. Kumar, M. U. M. Bhutta, and P. Zhi: J. King Saud Univ. – Comput. Inf. Sci. **34** (2022) 9060. https://doi.org/10.1016/j.jksuci.2022.08.031
33 V. B. Kolmanovskii and V. R. Nosov: Stability of Functional Differential Equations. (Academic Press, New York, 1986).
34 Q. Liang and J. M. Mendel: IEEE Trans. Fuzzy Syst. **8** (2000) 535. https://doi.org/10.1109/91.873577
35 L. X. Wang: Proc. 1992 IEEE Int. Conf. Fuzzy Systems (IEEE, 1992) 1163. https://doi.org/10.1109/FUZZY.1992.258721
36 P. Gahinet, A. Nemirovski, A. J. Laub, and M. Chilali: LMI Control Toolbox User's Guide (The MathWorks, Natick, 1995).

37 J. K. Hale and S. M. V. Lunel: On the Vanishing Viscosity Method for First Order Differential-functional IBVP (Springer-Verlag, New York, 1993).
38 X. Q. Huang and D. F. Huang: Ain Shams Eng. J. **14** (2022) 102029. https://doi.org/10.1016/j.asej.2022.102029